



All Theses and Dissertations

2010-04-14

Field Evaluation of Asphalt Overlays on State Route 30 in Northern Utah

Mark J. Butler

Brigham Young University - Provo

Follow this and additional works at: <https://scholarsarchive.byu.edu/etd>

 Part of the [Civil and Environmental Engineering Commons](#)

BYU ScholarsArchive Citation

Butler, Mark J., "Field Evaluation of Asphalt Overlays on State Route 30 in Northern Utah" (2010). *All Theses and Dissertations*. 2056.
<https://scholarsarchive.byu.edu/etd/2056>

This Thesis is brought to you for free and open access by BYU ScholarsArchive. It has been accepted for inclusion in All Theses and Dissertations by an authorized administrator of BYU ScholarsArchive. For more information, please contact scholarsarchive@byu.edu, ellen_amatangelo@byu.edu.

Field Evaluation of Asphalt Overlays on State Route 30 in Northern Utah

Mark Butler

A thesis submitted to the faculty of
Brigham Young University
in partial fulfillment of the requirements for the degree of
Master of Science

W. Spencer Guthrie, Chair
Mitsuru Saito
Grant G. Schultz

Department of Civil and Environmental Engineering
Brigham Young University
August 2010

Copyright © 2010 Mark Butler

All Rights Reserved

ABSTRACT

Field Evaluation of Asphalt Overlays on State Route 30 in Northern Utah

Mark Butler

Department of Civil and Environmental Engineering

Master of Science

The purpose of this research was to compare the rutting, cracking, and development of roughness of two asphalt overlay types commonly used in northern Utah and to evaluate how well the Mechanistic-Empirical Pavement Design Guide (MEPDG) can predict the observed results. AC-10 and PG 64-34 asphalt overlay materials were paved in a checkerboard pattern at a test site on State Route 30 near Logan, Utah, and observed for 3 years at 6-month intervals. Primary data included rutting, cracking, and roughness.

At the conclusion of the 3-year evaluation period, rut depths were 0.08 in. deeper, on average, in the AC-10 overlay compared to the PG 64-34 overlay. Fatigue cracking in the PG 64-34 overlay exceeded that in the AC-10 overlay by 0.11 percent, on average. The measured roughness of the PG 64-34 overlay was greater by 24 in./mile, on average, than the AC-10 overlay. In summary, although the AC-10 product exhibited more rutting than the PG 64-34 product, the latter exhibited more fatigue cracking and greater roughness than the former.

Although the MEPDG predictions for rutting are within the range of observed rut depths, the MEPDG overestimated the AC-10 rut depth while underestimating the PG 64-34 rut depth. Furthermore, the apparent inability of the MEPDG to predict amounts of longitudinal, fatigue, and transverse cracking comparable to measured values is concerning; the MEPDG predicted negligible cracking for both overlay types for the duration of the 3-year analysis period. While the MEPDG cracking models appear to be unsuitable for predicting cracking at this site, the MEPDG predictions for roughness are shown to be within the range of observed values.

Given the findings of this study, the researchers recommend that Utah Department of Transportation (UDOT) engineers consider specifying the AC-10 asphalt overlay product for pavement treatments in conditions similar to those evaluated in this investigation. Even though the MEPDG predictions of rutting and roughness were generally correct, the researchers recommend that such predicted values be used as general predictions only. Further evaluation of these models, as well as the MEPDG models for longitudinal, fatigue, and transverse cracking, should be completed before the MEPDG is fully adopted by UDOT.

Keywords: asphalt, overlay, mechanistic-empirical, MEPDG, rutting, cracking, roughness

ACKNOWLEDGMENTS

I am grateful to W. Spencer Guthrie for his dedication, direction, and mentorship from the beginning of this project. Without his hard work, experience, and genuine support, this report would not have been possible. I acknowledge the support of UDOT in funding this research. Also, special thanks to my father for his example in guiding me to civil engineering. This work is primarily dedicated to my dear wife for her loving support through the countless hours I devoted to this research

TABLE OF CONTENTS

| | |
|-----------------------------------------------|-----|
| TABLE OF CONTENTS..... | v |
| LIST OF TABLES | vii |
| LIST OF FIGURES | ix |
| 1 Introduction..... | 1 |
| 1.1 Problem Statement..... | 1 |
| 1.2 Scope..... | 3 |
| 1.3 Outline | 3 |
| 2 Background..... | 5 |
| 2.1 Overview..... | 5 |
| 2.2 Asphalt Overlay Composition | 5 |
| 2.2.1 Asphalt Binder | 5 |
| 2.2.2 Asphalt Concrete Aggregate..... | 6 |
| 2.3 Asphalt Overlay Performance..... | 7 |
| 2.3.1 Rutting..... | 7 |
| 2.3.2 Cracking..... | 8 |
| 2.3.3 Roughness..... | 11 |
| 2.4 Mechanistic-Empirical Overlay Design..... | 11 |
| 2.5 Summary..... | 12 |
| 3 Testing Procedures..... | 15 |
| 3.1 Overview..... | 15 |
| 3.2 Test Section Construction..... | 15 |
| 3.3 Field and Laboratory Testing..... | 17 |
| 3.3.1 Primary Data Collection | 18 |

| | | |
|-------|----------------------------------------------------------------------|----|
| 3.3.2 | Secondary Data Collection | 20 |
| 3.3.3 | Data Analyses | 24 |
| 3.4 | Numerical Modeling | 25 |
| 3.5 | Summary | 25 |
| 4 | Results | 27 |
| 4.1 | Overview | 27 |
| 4.2 | Testing | 27 |
| 4.2.1 | Data Reduction..... | 27 |
| 4.2.2 | Regression Analyses | 33 |
| 4.3 | Numerical Modeling..... | 36 |
| 4.4 | Summary | 42 |
| 5 | Conclusion | 45 |
| 5.1 | Summary | 45 |
| 5.2 | Findings | 46 |
| 5.3 | Recommendations..... | 48 |
| | References..... | 49 |
| | APPENDIX A: Raw Data..... | 53 |
| | APPENDIX B: Results of Statistical Analyses | 67 |
| | APPENDIX C: Mechanistic-Empirical Pavement Design Guide Inputs | 71 |

LIST OF TABLES

| | | |
|------------|--------------------------------------------------|----|
| Table 2.1 | UDOT IRI Ratings..... | 11 |
| Table 3.1 | Testing Schedule..... | 18 |
| Table 4.1 | Rutting Data..... | 28 |
| Table 4.2 | Longitudinal Cracking Data..... | 28 |
| Table 4.3 | Transverse Cracking Data..... | 28 |
| Table 4.4 | Fatigue Cracking Data..... | 28 |
| Table 4.5 | Roughness Data..... | 29 |
| Table 4.6 | Temperatures Measured during Testing..... | 29 |
| Table 4.7 | Base and Subgrade California Bearing Ratios..... | 30 |
| Table 4.8 | Asphalt Material Properties..... | 32 |
| Table 4.9 | Asphalt Layer Thicknesses..... | 33 |
| Table 4.10 | Results of Statistical Analyses..... | 34 |

LIST OF FIGURES

| | | |
|-------------|-----------------------------------------------------------|----|
| Figure 2.1 | Rutting..... | 8 |
| Figure 2.2 | Longitudinal Cracking | 9 |
| Figure 2.3 | Transverse Cracking | 9 |
| Figure 2.4 | Fatigue Cracking..... | 10 |
| Figure 3.1 | Aerial View of State Route 30 near Logan, Utah..... | 15 |
| Figure 3.2 | Irrigation Canal along Westbound State Route 30 | 16 |
| Figure 3.3 | Milling of Existing Asphalt Surface | 17 |
| Figure 3.4 | Configuration of Test Sections | 17 |
| Figure 3.5 | Measurement of Rut Depth..... | 19 |
| Figure 3.6 | Measurement of Roughness..... | 20 |
| Figure 3.7 | Measurement of Penetration Rate..... | 21 |
| Figure 3.8 | Measurement of Electrical Properties..... | 22 |
| Figure 3.9 | Coring of Asphalt Layer | 23 |
| Figure 4.1 | Penetration Rate Profiles..... | 30 |
| Figure 4.2 | Dielectric Value Profiles..... | 31 |
| Figure 4.3 | Electrical Conductivity Profiles..... | 31 |
| Figure 4.4 | Typical Core Sample..... | 32 |
| Figure 4.5 | Aggregate Gradations for Asphalt Layers | 33 |
| Figure 4.6 | Observed and Modeled Trends in Rut Depth | 37 |
| Figure 4.7 | Observed and Modeled Trends in Longitudinal Cracking..... | 38 |
| Figure 4.8 | Observed and Modeled Trends in Transverse Cracking..... | 38 |
| Figure 4.9 | Observed and Modeled Trends in Fatigue Cracking | 39 |
| Figure 4.10 | Observed and Modeled Trends in Roughness | 39 |

1 INTRODUCTION

1.1 Problem Statement

Roadway managers are constantly faced with the challenge of maintaining rapidly deteriorating roadways with limited funding. A common and comparatively inexpensive method of roadway rehabilitation is placement of an asphalt overlay. The additional pavement life provided by the overlay depends to a great degree on the properties of the asphalt material itself, while the accuracy of pavement life prediction depends on the adequacy of design and analysis tools available in the industry for this purpose.

The properties of the asphalt overlay for a given project should be specified based on the expected traffic loading and climatic conditions for the pavement system. Since the Utah Department of Transportation (UDOT) adopted the Superpave mixture design protocols developed in the 1990s, UDOT engineers have typically used a performance-graded PG 64-34 binder with a 0.5-in. nominal maximum aggregate size in overlay materials. Previously, particularly in northern Utah, a viscosity-graded AC-10 binder with a 0.375-in. nominal maximum aggregate size had been typically specified for overlays.

Because some UDOT maintenance engineers have indicated a strong preference for the older product, citing anecdotal evidence of its superiority over the PG 64-34 material in cold regions, UDOT engineers contracted with researchers at Brigham Young University (BYU) to investigate the performance of these two types of asphalt overlays and to evaluate the utility of

the new mechanistic-empirical pavement design guide (MEPDG) software for predicting overlay performance. With the primary objectives of comparing the PG 64-34 and AC-10 overlay materials commonly used in northern Utah and evaluating the ability of the MEPDG to predict performance, this research will therefore be helpful not only to UDOT pavement managers but also to other members of the pavement industry whose jurisdictions have similar traffic conditions, underlying pavement structure, and climatic conditions.

Past research performed in this area has focused primarily on asphalt binder performance in laboratory testing (1, 2). One such study, performed by the Virginia Department of Transportation (VDOT), aimed to compare the performance of AC-20 and AC-30 binders against PG 76-22, PG 70-22, and PG 64-22 binders in the laboratory. VDOT researchers found that the PG binders outperformed the AC binders in all areas (3). Other research was performed to investigate the contribution of maximum aggregate size to rutting potential in an asphalt concrete mix (4). Brown et al. found that larger maximum aggregate sizes increased the Marshall stability of an asphalt concrete mix and reduced the overall rutting potential (5). Button et al. confirmed Brown's findings in a laboratory study that replaced coarse aggregates with fines. A mix with more fine aggregates was found to exhibit a larger rutting potential (6). Investigations of field performance were not conducted in either study.

Regarding performance predictions, the literature contains various sensitivity studies conducted on the new MEPDG (7, 8, 9), but few field validations have been published. However, one recent UDOT study was performed to calibrate the MEPDG to typical Utah climate conditions using data from the UDOT pavement management system and the Long-Term Pavement Performance (LTPP) Program data. This study suggested that the MEPDG reasonably predicted all types of distress except for rutting. The study suggests that further MEPDG

validation be performed on hot mix asphalt (HMA) pavements (10). The Minnesota Department of Transportation (MDT) conducted a similar study. This research found that the MEPDG reasonably predicted all types of distress except for longitudinal cracking (11). Given the apparent inconsistencies in these findings, further research is needed to evaluate the ability of the MEPDG to perform accurate distress predictions for asphalt overlays in northern Utah.

1.2 Scope

To facilitate a direct comparison of products, both the PG 64-34 and AC-10 asphalt overlay materials were used to pave selected portions of State Route 30 (SR-30) near Logan, Utah. At the request of UDOT engineers, who were responsible for the site selection, materials selection, experimental design, and construction contracts, BYU researchers conducted a comprehensive field evaluation of pavement conditions at the site over a 3-year period. Evaluations included rutting, cracking, and roughness surveys, as well as structural testing and sampling to characterize the pavement layers. Performance predictions were developed for these overlays using the MEPDG, and their predicted values were compared against the measured field data.

1.3 Outline

This report contains five chapters. Chapter 1 describes the problem statement and scope, while Chapter 2 presents background information on asphalt concrete overlays. Chapter 3 provides a detailed description of the test procedures. Chapter 4 includes results associated with the observed and modeled data, and Chapter 5 presents conclusions of the study and recommendations for further research.

2 BACKGROUND

2.1 Overview

This chapter discusses asphalt overlay composition and performance, as well as the mechanistic-empirical (M-E) overlay design approach.

2.2 Asphalt Overlay Composition

Asphalt overlays, like conventional asphalt concrete pavement layers, consist of asphalt cement binder and aggregates. The asphalt cement acts as the glue that binds aggregates together. For production of asphalt concrete that is suitable for a given pavement, various binder types and aggregate gradations can be used to accommodate site-specific traffic loading and environmental conditions. The following sections provide a brief description of each of these components of asphalt concrete in overlays.

2.2.1 Asphalt Binder

The performance of an asphalt overlay depends to a large degree on the type of binder utilized in the overlay material. Because binder viscosity depends heavily on temperature, the challenge behind specifying the correct binder type lies in matching the binder to the climatic conditions at the project site. In cold regions, a soft binder not susceptible to thermal cracking

would be needed, while in hot climates a hard binder would be needed to resist rutting and shoving under traffic loading (12).

Asphalt binder grading systems have been developed to aid asphalt overlay mix designers in selecting the proper binder. The AC system classifies binders based on the viscosity of the neat asphalt cement measured at 60°C (13). However, this system does not evaluate cold-temperature behavior, a need addressed in the more recently developed PG system utilizing more rigorous testing criteria (12, 14). From the outset, the PG specification proved so useful that the Federal Highway Administration (FHWA) sought nationwide adoption of the PG binder specification system by 1997 (3). UDOT engineers adopted the PG system by 1997 and have seldom used anything but PG mixes since that time.

2.2.2 Asphalt Concrete Aggregate

Aggregate properties important to overlays include aggregate shape, surface condition, and gradation. Angular aggregates provide greater internal friction, which results in greater mechanical stability than can generally be achieved using rounded aggregates. A rough surface condition not only increases internal friction but also provides an improved bond with the asphalt cement binder. Gradation is perhaps the most important property of an aggregate because it affects stiffness, stability, durability, permeability, fatigue resistance, frictional resistance, and resistance to moisture damage (4). These factors, in turn, affect the resistance of the asphalt overlay to rutting, cracking, and the development of roughness.

The nominal maximum size of aggregate used in an overlay is generally smaller than that used in thicker conventional asphalt concrete layers. The nominal maximum aggregate size is typically no larger than half the lift thickness (4). Because a lift of conventional asphalt paving is between 2 and 4 in. thick, the nominal maximum aggregate size can be quite large. However,

with typical asphalt overlay thicknesses ranging from 1 to 2 in., the nominal maximum aggregate size is limited to 0.5 to 1 in. Given the findings of researchers that the use of larger aggregates provides greater resistance to rutting, one may expect asphalt overlays to be more susceptible to rutting, on average, than conventional asphalt lifts (5). However, the use of smaller aggregates in the wearing course typically provides a smoother pavement surface for the traveling public (15).

2.3 Asphalt Overlay Performance

In this research, asphalt overlay performance is defined as resistance to rutting, cracking, and the development of roughness, each of which is addressed in the following sections. Raveling, shoving, heaving, polishing, bleeding, and other distresses defined in the LTPP Program are outside the scope of this research (16).

2.3.1 Rutting

Rutting is defined as permanent deformation of the pavement surface as a result of subsurface material consolidation and/or lateral shoving of asphalt surface layers under traffic loading. Rutting can be visually identified in the wearing course as a longitudinal depression in the wheel paths (17). Rutting may be more visible after rainfall due to the accumulation of water in the depressions. Severe rutting poses a safety concern because, as rut depth increases, a vehicle is more likely to hydroplane during a severe rain event. An example of rutting is shown in Figure 2.1.



Figure 2.1 Rutting

2.3.2 Cracking

Longitudinal, transverse, and fatigue cracking are common modes of asphalt overlay deterioration. Longitudinal cracking is defined as cracking predominately parallel to the pavement centerline (16). Longitudinal cracking that occurs in a wheel path is generally load-induced, while similar cracking outside a wheel path is often caused by thermal effects. An example of longitudinal cracking is shown in Figure 2.2. Transverse cracking is defined as cracking predominately perpendicular to the pavement centerline (16). Transverse cracking is caused by thermal expansion and contraction due to rapid temperature changes. An example of transverse cracking is shown in Figure 2.3.



Figure 2.2 Longitudinal Cracking



Figure 2.3 Transverse Cracking

Fatigue cracking is a series of interconnected cracks caused by fatigue failure of the asphalt surface course under traffic loading (16). Fatigue cracks begin at the bottom surface of the wearing course and propagate upward under repeated wheel loading. As depicted in Figure 2.4, the cracks initially form parallel to each other in a wheel path and then interconnect under continued loading to form a pattern that resembles that on the back of an alligator. For this reason, fatigue cracking is often called “alligator” cracking.

The very presence of fatigue, longitudinal, and transverse cracking can cause attendant reductions in the overall ride quality of a pavement, and the rate of deterioration of the pavement structure will increase if the cracks are not regularly sealed. Unsealed cracks allow water ingress into the subsurface layers, leading to potential softening of the base materials and reduced support of the asphalt layer.



Figure 2.4 Fatigue Cracking

2.3.3 Roughness

Roughness is a measure of overall ride quality, commonly quantified in terms of the International Roughness Index (IRI). IRI is defined as the average rectified slope (ARS), which is the ratio of the accumulated suspension motion to the distance traveled obtained from the mathematical model of a standard quarter car transversing a measured profile at a speed of 50 mph (17). A standard quarter car is a theoretical model that uses a spring and a dashpot to model suspension motion. IRI classifications published by UDOT are shown in Table 2.1 (18). High IRI values correspond to low ride quality, which can be caused by the presence of pavement distress as described previously.

Table 2.1 UDOT IRI Ratings

| Pavement Type | International Roughness Index (in./mile) | | | | |
|--------------------|------------------------------------------|-----------|------------|------------|------------|
| | Very Good | Good | Fair | Poor | Very Poor |
| Interstate Asphalt | 30 to 50 | 50 to 90 | 90 to 130 | 130 to 170 | 170 to 230 |
| High-Speed Asphalt | 33 to 55 | 55 to 97 | 97 to 140 | 140 to 182 | 182 to 247 |
| Mid-Speed Asphalt | 37 to 60 | 60 to 105 | 105 to 150 | 150 to 195 | 195 to 262 |
| Low-Speed Asphalt | 41 to 65 | 65 to 112 | 112 to 160 | 160 to 207 | 207 to 278 |

2.4 Mechanistic-Empirical Overlay Design

The accuracy of pavement life prediction depends on the adequacy of design and analysis tools available in the industry for this purpose. In the past, overlay design has been performed using empirical equations derived from the American Association of State Highway Officials (AASHO) road test of the 1950s (17). The reality of using a road test for the basis of developing a design guide is that use of the guide for conditions outside the scope of the road test requires extrapolation, which may limit the utility of the guide in such circumstances. While desirable, constructing test roads for all situations is not possible due to both time and funding constraints;

therefore, development and validation of a comprehensive computer model for predicting pavement performance would be beneficial to the pavement industry.

Under National Cooperative Highway Research Program (NCHRP) 1-37A and 1-40D, an M-E approach to pavement design and analysis was developed. The mechanistic part of the new MEPDG methodology involves computation of stresses and/or strains at specified depths in the pavement structure, with traffic loading, material properties, and climatic conditions as inputs. The empirical part of the methodology involves relating the computed stresses and/or strains to pavement life through transfer functions developed for that purpose. The MEPDG considers fatigue and longitudinal cracking to be primarily due to traffic loading and thermal or transverse cracking to be primarily due to climatic factors. Analyses performed using the MEPDG involve complex models with numerous inputs describing information about the project, traffic, weather, general pavement structure, wearing course structure, existing asphalt structure, base structure, and subgrade structure (19).

2.5 Summary

In summary, asphalt overlays, like conventional asphalt concrete pavement layers, consist of asphalt cement binder and aggregates. Various binder types and aggregate gradations are used to accommodate site-specific traffic loading and environmental conditions. Two common binder grading systems include the AC viscosity grading system and the PG system. Aggregate properties important to overlays include aggregate shape, surface condition, and gradation.

Asphalt overlay performance can be defined as resistance to rutting, cracking, and the development of roughness. Rutting is defined as permanent deformation of the pavement surface as a result of subsurface material consolidation and/or lateral shoving of asphalt surface layers

under traffic loading. Fatigue cracking is a series of interconnected cracks caused by fatigue failure of the asphalt surface course under traffic loading. Longitudinal and transverse cracking are defined as cracking predominately parallel and perpendicular to the pavement centerline, respectively. Roughness is a measure of overall ride quality, commonly quantified in terms of the IRI; high IRI values correspond to low ride quality, which can be caused by the presence of pavement distress.

The new MEPDG methodology allows for analyses of overlay performance. Analyses performed using the MEPDG involve complex models with numerous inputs describing information about the project, traffic, weather, general pavement structure, wearing course structure, existing asphalt structure, base structure, and subgrade structure.

3 TESTING PROCEDURES

3.1 Overview

This research involved construction of field test sections, field and laboratory testing, and numerical modeling of pavement performance as described in the following sections.

3.2 Test Section Construction

The test sections evaluated in this research were constructed in July 2006 on SR-30 west of Logan, Utah, between mile posts 104 and 107; Figure 3.1 shows an aerial view of the site. At this location, SR-30 consists of two lanes oriented in the east-west direction with irrigation canals along both sides of the road. The canal on the north side of the road remains full for most of the spring and summer as shown in Figure 3.2, while the canal on the south side remains



Figure 3.1 Aerial View of State Route 30 near Logan, Utah



Figure 3.2 Irrigation Canal along Westbound State Route 30

empty. The water table depth at the site is 4.5 ft according to a 2006 U.S. Department of Agriculture soil survey (20).

As shown in Figure 3.3, the surface of the road was initially milled to remove deteriorated chip seals and to provide a similar texture through the entire experimental area. After the milling was complete and the milled surface was broomed, the PG 64-34 and AC-10 asphalt overlay materials were paved in a checkerboard pattern such that drivers encountered the AC-10 product first when traveling in either direction. Twenty test stations were randomly selected along each of the east and west segments of the roadway, and survey-grade nails were installed in the pavement surface so that repeated testing could be performed at the same locations. Figure 3.4 shows the general layout of the site.



Figure 3.3 Milling of Existing Asphalt Surface

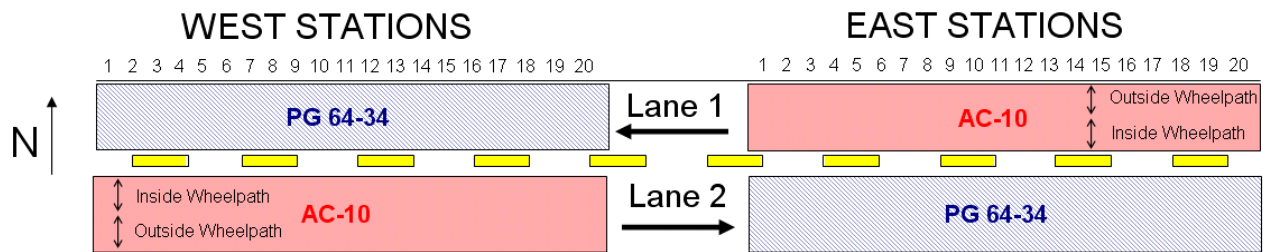


Figure 3.4 Configuration of Test Sections

3.3 Field and Laboratory Testing

Field testing involved returning to the site on approximately 6-month intervals to collect specific data from each pavement section. In particular, rut depth, cracking, roughness, modulus, and layer thickness data were collected following the schedule shown in Table 3.1. Data were collected for two purposes. Rut depth, cracking, and roughness data were primarily collected to facilitate a direct comparison of the performance of the two overlays, while material properties

Table 3.1 Testing Schedule

| Trip Number | Trip Date | Type of Testing | | | | |
|-------------|---------------|-----------------|----------|-----------|---------|-----------------|
| | | Rut Depth | Cracking | Roughness | Modulus | Layer Thickness |
| 1 | December 2006 | X | X | | | |
| 2 | June 2007 | X | X | | | |
| 3 | November 2007 | X | X | | | |
| 4 | May 2008 | X | X | | | |
| 5 | October 2008 | X | X | X | X | X |
| 6 | July 2009 | X | X | X | | X |

and layer thicknesses were evaluated as secondary data to investigate the uniformity of subsurface conditions and for use in MEPDG analyses of the test sites.

As shown in Table 3.1, rut depth testing and cracking surveys were performed during all visits. Roughness was measured only during the last two trips because a roadway profiler was not available previous to that time. Modulus values were measured in early fall, an appropriate time to obtain values representative of average annual conditions (17). Discussions of procedures utilized to collect both the primary and secondary data required in this research are provided in the following subsections.

3.3.1 Primary Data Collection

Primary data included rutting, cracking, and roughness. Rutting was measured following ASTM E1703 (Standard Test Method for Measuring Rut-Depth of Pavement Surfaces Using a Straightedge) at each of the 20 test stations in each of the four experimental sections. Researchers placed a ruled 6-ft level perpendicular to the roadway centerline, spanning inside and outside wheel paths in turn. A separate ruler held in the vertical direction was then used to measure to the nearest 1 mm the point of deepest rutting within each wheel path, as illustrated in Figure 3.5; any debris present on the pavement surface at the contact points was brushed away to



Figure 3.5 Measurement of Rut Depth

ensure valid readings. The width of rutting in each wheel path was also recorded to the nearest 1 in. (The use of metric units for measuring rut depth is convenient, as it involves whole numbers, and it is also consistent with the LTPP Program protocols. However, in this research, the rut depths were later converted to units of inches for analysis.)

Cracking data were collected in general accordance with the protocols outlined for the LTPP Program (16). Researchers performed a walking survey of each pavement section while recording the type, length or area, and severity level of observed cracking. Cracking data were reported as total length of longitudinal and transverse cracking in feet and total area of fatigue cracking in square feet. These data were collected for each test section as a whole; cracking data were not measured by station.

As shown in Figure 3.6, roughness data were collected in the outside wheel path at each of the 20 test stations using a dipstick roadway profiler. Each test line was 40 ft in length, beginning 20 ft before the station marker and ending 20 ft past the station marker. With each



Figure 3.6 Measurement of Roughness

step, the dipstick recorded the grade slope and then computed an IRI value in units of inches per mile from the slope variance associated with the given survey (16). Air and pavement surface temperatures at the time of testing were also collected as part of the primary data set.

The collected data were then reduced for analysis. Average rut depths, fatigue cracking percentages, lengths of longitudinal and transverse cracks, and IRI values were computed for each section for each site visit. The data were also plotted against time so that temporal trends could be evaluated.

3.3.2 Secondary Data Collection

Secondary data included dynamic cone penetrometer (DCP) test results, dielectric and electrical conductivity profiles, and core information. As shown in Figure 3.7, the DCP consists of a slide-hammer assembly mounted to a shaft fitted with a standard cone tip. For this research,



Figure 3.7 Measurement of Penetration Rate

a 1.5-in.-diameter hole was drilled through the asphalt layer at each test station to facilitate DCP testing of the subsurface layers to a depth of approximately 35 in.

After a given set of blows, the total penetration depth of the cone tip was measured, and incremental penetration rates were then calculated. Contrasts in mechanical properties of adjacent layers caused changes in penetration rates with depth and allowed estimation of layer thicknesses. In addition, the average penetration rate in a given layer was used to calculate the California bearing ratio (CBR) for that layer according to Equation 3.1:

$$CBR = \frac{292}{DCP^{1.12}} \quad (3.1)$$

where: CBR = California bearing ratio

DCP = penetration rate, mm/blow

CBR values were then correlated to modulus values, as required, using standard charts (17).

After a DCP test was completed, a 1-in.-diameter bull pick was hammered into the DCP hole to a depth of approximately 35 in. and then removed using a high-lift jack. A downhole probe capable of measuring both dielectric value and electrical conductivity probe was then fully inserted into the hole as shown in Figure 3.8, and readings were obtained on 1-in. intervals from the depth of insertion to approximately the middle of the asphalt layer. Because dielectric and electrical conductivity values are sensitive to both soil type and moisture content, these data were useful supplements to the DCP data for determining layer thicknesses.

One asphalt core sample was removed from each pavement section using a truck-mounted coring rig as depicted in Figure 3.9. Coring allowed a direct measurement of the asphalt layer thickness and facilitated laboratory testing of the in-situ material. After the core



Figure 3.8 Measurement of Electrical Properties



Figure 3.9 Coring of Asphalt Layer

was removed, a small sample of the base and subgrade was removed to generally characterize each layer.

Asphalt cores were transported to the BYU Highway Materials Laboratory for unit weight, specific gravity, asphalt content, and aggregate gradation testing. As required to obtain data for the MEPDG analysis, each core was cut horizontally at the interface between the most recent overlay and the underlying asphalt layers, and the bottom face of each core was trimmed flat. The weight, diameter, and height of each piece were then measured to facilitate calculation of unit weight. Specific gravity testing was performed following American Association for State Highway Transportation Officials AASHTO T 209 (Theoretical Maximum Specific Gravity and Density of Hot Mix Asphalt (HMA) Paving Mixtures), and asphalt content was determined in accordance with AASHTO T 308 (Standard Method of Test for Determining the Asphalt Binder Content of HMA by the Ignition Method). A sieve analysis following AASHTO T 27 (Sieve

Analysis for Fine and Coarse Aggregates) was then performed on the aggregate remaining from the ignition testing.

3.3.3 Data Analyses

Following data collection and reduction, the effects of several factors on the performance of the overlay products were investigated using statistical software. Factors of interest included overlay type, lane direction, asphalt thickness, base thickness, and base and subgrade CBR values. While overlay type was controlled in this research, the total asphalt thickness, base thickness, and base and subgrade CBR values could not be controlled; the values of these properties were measured, however, so that these factors could be accounted for in the regression analyses performed on the data. Features connected to lane direction included traffic loading and the effects of the canal water, which also could not be controlled.

A stepwise regression analysis was performed to determine the most significant predictor variables for each of the five response variables of interest in this research: rutting, fatigue cracking, longitudinal cracking, transverse cracking, and roughness. In a stepwise regression process, the utility of potential predictor variables is assessed using a p -value, or level of significance, computed for each variable. The predictor variables found to be the most influential on the response variable are used in the formation of the regression model. In this research, predictor variables having p -values less than or equal to 0.15 were included in the regression models. Once a given regression model is formed, a coefficient of determination, or R^2 value, can be computed for the model. The R^2 value reflects the percentage of variation in the response variable that is explained by variation in the predictor variables included in the regression model, where an R^2 value of 1.0 represents a perfect model (21).

3.4 Numerical Modeling

Numerical modeling was performed in this research using the MEPDG. One analysis was performed for each type of asphalt overlay material, and, where possible, values for the numerous inputs were determined specifically for the field sections investigated in this research. Inputs included information about the project, traffic, weather, general pavement structure, wearing course structure, existing asphalt structure, base structure, and subgrade structure.

While project and pavement structural data could generally be determined by research personnel from field measurements, much of the traffic data were provided by UDOT engineers. Data downloaded from the Logan Municipal Airport weather station, which is located less than 5 miles from the project site, were used to characterize climatic conditions. For variables not specifically measured, default values were accepted. Because time and funding constraints apply to many projects, lack of complete data sets is a common challenge. The MEPDG therefore provides a hierarchy of input levels from 1 to 3, where levels 1 and 3 involve the highest and lowest levels of detail, respectively. In this research, input levels 2 and 3 were utilized (20). The results of the MEPDG simulations were then compared to the values of rutting, fatigue cracking, longitudinal cracking, transverse cracking, and roughness measured in the field to evaluate the ability of the MEPDG to predict asphalt overlay performance.

3.5 Summary

The test sections evaluated in this research were constructed in July 2006 on SR-30 west of Logan, Utah, between mile posts 104 and 107. At this location, SR-30 consists of two lanes oriented in the east-west direction with irrigation canals along both sides of the road. PG 64-34

and AC-10 asphalt overlay materials were paved in a checkerboard pattern at the site, and 20 test stations were randomly selected along each of the east and west segments of the roadway.

Field testing involved returning to the site on approximately 6-month intervals to collect specific data from each pavement section. Primary data included rutting, cracking, and roughness, which were collected to facilitate a direct comparison of the performance of the two overlays. Material properties and layer thicknesses were evaluated as secondary data to investigate the uniformity of subsurface conditions and for use in MEPDG analyses of the test sites.

Following data collection and reduction, the effects of several factors on the performance of the overlay products at the conclusion of the 3-year testing period were investigated using statistical software. Factors of interest included overlay type, lane direction, asphalt thickness, base thickness, and base and subgrade CBR values. A stepwise regression analysis was performed to determine the most significant predictor variables for each of the five response variables of interest in this research: rutting, fatigue cracking, longitudinal cracking, transverse cracking, and roughness.

Numerical modeling was then performed using the MEPDG. One analysis was performed for each type of asphalt overlay material, and values for the numerous inputs were determined specifically for the field sections investigated in this research. The results of the MEPDG simulations were then compared to the values of rutting, fatigue cracking, longitudinal cracking, transverse cracking, and roughness measured in the field.

4 RESULTS

4.1 Overview

The following sections present the results of this research, including those derived from testing and numerical modeling. These results are specific to the pavement structural characteristics, traffic loading, and climatic conditions present along the project corridor.

4.2 Testing

The results of testing include data reduction and data analyses as described in the following sections. The data were collected to enable comparison of the performance of the AC-10 and PG 64-34 overlay materials and to facilitate the MEPDG analyses.

4.2.1 Data Reduction

Tables 4.1 to 4.5 display summaries of rutting, longitudinal cracking, transverse cracking, fatigue cracking, and roughness data, respectively. Given the deliberate lack of maintenance treatments on the experimental sections, the quantity of distress should increase monotonically through time; slight aberrations evident in some of the temporal trends are probably attributable to operator variability in measuring. Statistical analyses of the primary data, as well as plots of the trends, are provided in subsequent sections, and all of the raw data are provided in Appendix A. Temperatures measured during field testing are shown in Table 4.6. Although three data

Table 4.1 Rutting Data

| Asphalt Type | Lane Direction | Average Rut Depth (in.) | | | | | |
|--------------|----------------|-------------------------|-----------|---------------|----------|--------------|-----------|
| | | December 2006 | June 2007 | November 2007 | May 2008 | October 2008 | July 2009 |
| AC | EB | 0.12 | 0.10 | 0.16 | 0.14 | 0.16 | 0.18 |
| | WB | 0.15 | 0.15 | 0.21 | 0.20 | 0.22 | 0.24 |
| PG | EB | 0.12 | 0.08 | 0.11 | 0.11 | 0.12 | 0.11 |
| | WB | 0.11 | 0.06 | 0.11 | 0.12 | 0.12 | 0.16 |

Table 4.2 Longitudinal Cracking Data

| Asphalt Type | Lane Direction | Total Longitudinal Crack Length (ft) | | | | | |
|--------------|----------------|--------------------------------------|-----------|---------------|----------|--------------|-----------|
| | | December 2006 | June 2007 | November 2007 | May 2008 | October 2008 | July 2009 |
| AC | EB | 0 | 0 | 8 | 95 | 148 | 768 |
| | WB | 0 | 0 | 25 | 125 | 194 | 455 |
| PG | EB | 0 | 0 | 0 | 128 | 237 | 509 |
| | WB | 0 | 0 | 4 | 480 | 440 | 1747 |

Table 4.3 Transverse Cracking Data

| Asphalt Type | Lane Direction | Total Transverse Crack Length (ft) | | | | | |
|--------------|----------------|------------------------------------|-----------|---------------|----------|--------------|-----------|
| | | December 2006 | June 2007 | November 2007 | May 2008 | October 2008 | July 2009 |
| AC | EB | 0 | 0 | 64 | 62 | 219 | 333 |
| | WB | 0 | 0 | 178 | 336 | 523 | 749 |
| PG | EB | 0 | 0 | 17 | 122 | 237 | 338 |
| | WB | 0 | 0 | 0 | 96 | 201 | 254 |

Table 4.4 Fatigue Cracking Data

| Asphalt Type | Lane Direction | Average Fatigued Area (%) | | | | | |
|--------------|----------------|---------------------------|-----------|---------------|----------|--------------|-----------|
| | | December 2006 | June 2007 | November 2007 | May 2008 | October 2008 | July 2009 |
| AC | EB | 0.00 | 0.00 | 0.00 | 0.00 | 0.03 | 0.23 |
| | WB | 0.00 | 0.00 | 0.00 | 0.03 | 0.00 | 0.00 |
| PG | EB | 0.00 | 0.00 | 0.00 | 0.00 | 0.00 | 0.00 |
| | WB | 0.00 | 0.00 | 0.00 | 0.18 | 0.22 | 0.41 |

Table 4.5 Roughness Data

| Asphalt Type | Lane Direction | IRI (in./mile) | | | | | |
|--------------|----------------|----------------|-----------|---------------|----------|--------------|-----------|
| | | December 2006 | June 2007 | November 2007 | May 2008 | October 2008 | July 2009 |
| AC | EB | - | - | - | - | 94 | 97 |
| | WB | - | - | - | - | 85 | 92 |
| PG | EB | - | - | - | - | 99 | 110 |
| | WB | - | - | - | - | 117 | 129 |

Table 4.6 Temperatures Measured during Testing

| | Temperature (°F) | | | | | |
|------------------|------------------|-----------|---------------|----------|--------------|-----------|
| | December 2006 | June 2007 | November 2007 | May 2008 | October 2008 | July 2009 |
| Ambient Air | 58 | 80 | - | 58 | 40 | 73 |
| Pavement Surface | 51 | - | - | 43 | 45 | 55 |

points were not obtained during field work, as indicated by hyphens in the table, the measured pavement surface temperatures, in particular, are so similar to each other that variations in measured crack widths due to pavement surface temperature were probably not significant. Table 4.7 shows the CBR values computed for the base and subgrade materials at each test location. Figures 4.1 to 4.3 display the results of DCP, dielectric value, and electrical conductivity tests, respectively. The DCP penetration rates and both electrical profiles display an interface between the base and subgrade layers at a depth of approximately 22 in. below the pavement surface. The base layer, in particular, was found to be extremely stiff; significant effort was required to penetrate it with the DCP apparatus. From the measured material properties and inspection of the limited samples removed from the pavement structure during coring, the base and subgrade materials were determined to be densely compacted river gravel and clayey soil, respectively.

Table 4.7 Base and Subgrade California Bearing Ratios

| Pavement Layer | Asphalt Type | Lane Direction | Average Penetration Rate (in./blow) | Average CBR |
|----------------|--------------|----------------|-------------------------------------|-------------|
| Base | AC | EB | 0.08 | 153 |
| | | WB | 0.06 | 223 |
| | PG | EB | 0.08 | 189 |
| | | WB | 0.24 | 59 |
| Subgrade | AC | EB | 0.73 | 17 |
| | | WB | 0.68 | 17 |
| | PG | EB | 0.81 | 15 |
| | | WB | 0.56 | 28 |

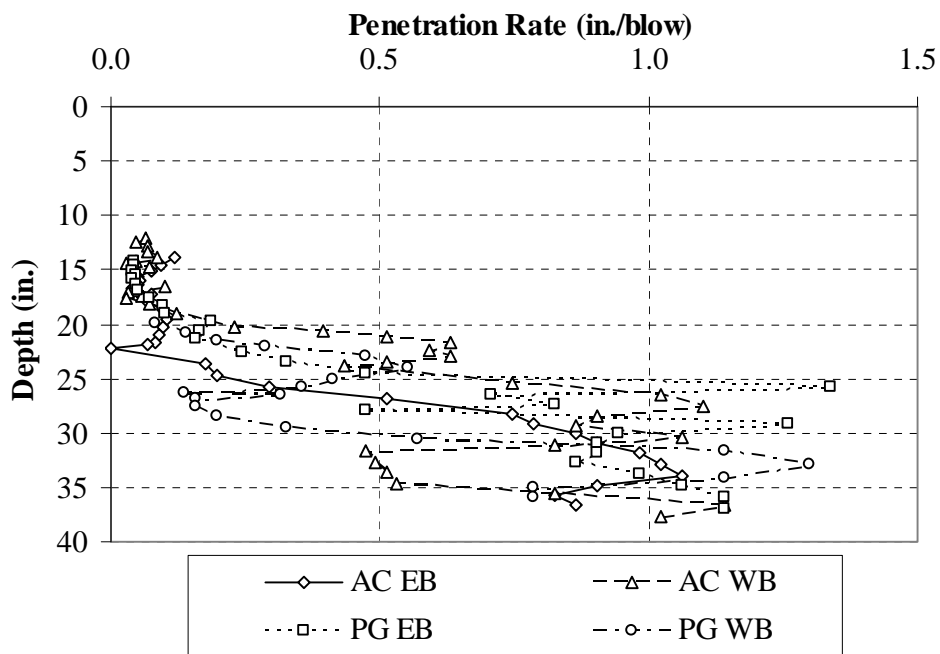


Figure 4.1 Penetration Rate Profiles

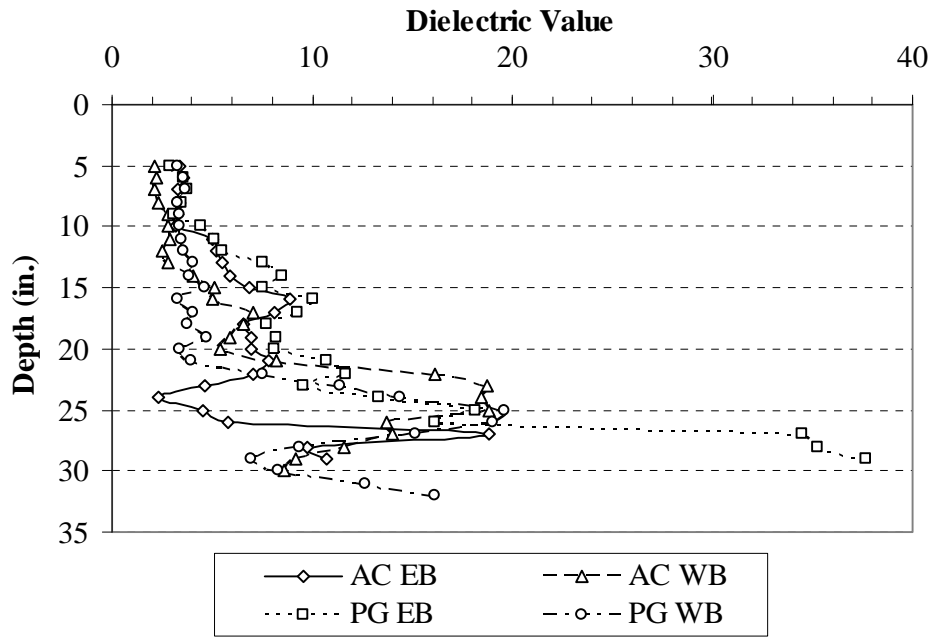


Figure 4.2 Dielectric Value Profiles

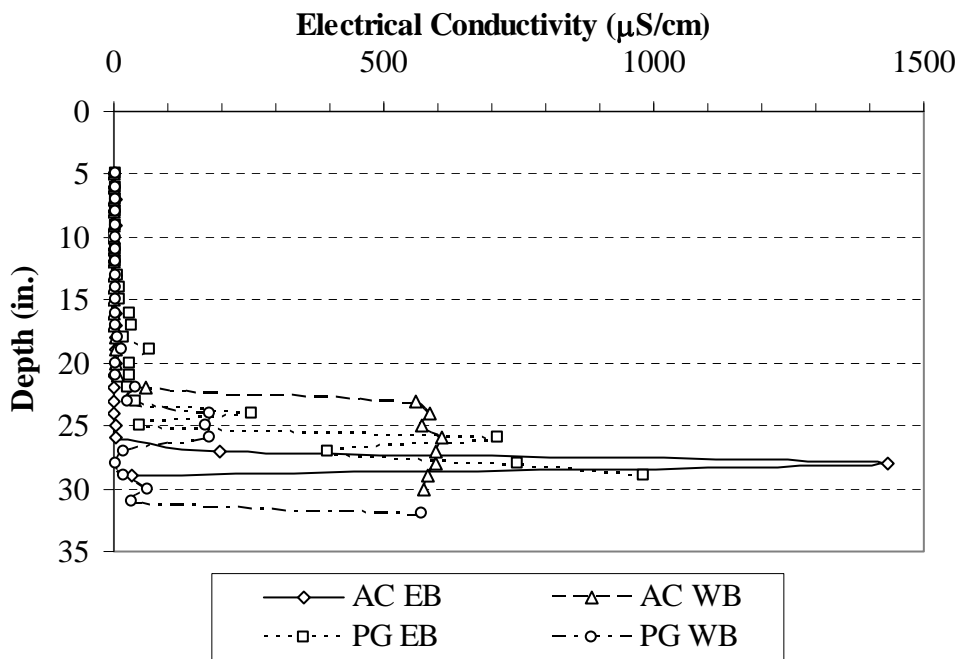


Figure 4.3 Electrical Conductivity Profiles

Cores removed from the test sections clearly indicated that the roadway had been overlaid several times; multiple asphalt layers are evident in the typical core sample shown in Figure 4.4. Layer thicknesses are provided in Table 4.8, and material properties determined from the core samples are given in Table 4.9. The results of the sieve analyses are shown in Figure 4.5.



Figure 4.4 Typical Core Sample

Table 4.8 Asphalt Material Properties

| Asphalt Layer | SG | Air (%) | Unit Weight (pcf) | Asphalt Content (%) |
|------------------|------|---------|-------------------|---------------------|
| AC-10 Overlay | 2.41 | 3.6 | 144.9 | 5.1 |
| PG 64-34 Overlay | 2.42 | 7.7 | 139.3 | 4.9 |
| Existing Asphalt | 2.33 | 3.9 | 139.5 | 6.3 |

Table 4.9 Asphalt Layer Thicknesses

| Asphalt Layer | Asphalt Type | Lane Direction | Layer Thickness (in.) |
|------------------|--------------|----------------|-----------------------|
| Overlay Asphalt | AC | EB | 1.8 |
| | | WB | 2.3 |
| | PG | EB | 2.3 |
| | | WB | 2.3 |
| Existing Asphalt | AC | EB | 11.0 |
| | | WB | 8.3 |
| | PG | EB | 11.8 |
| | | WB | 8.3 |

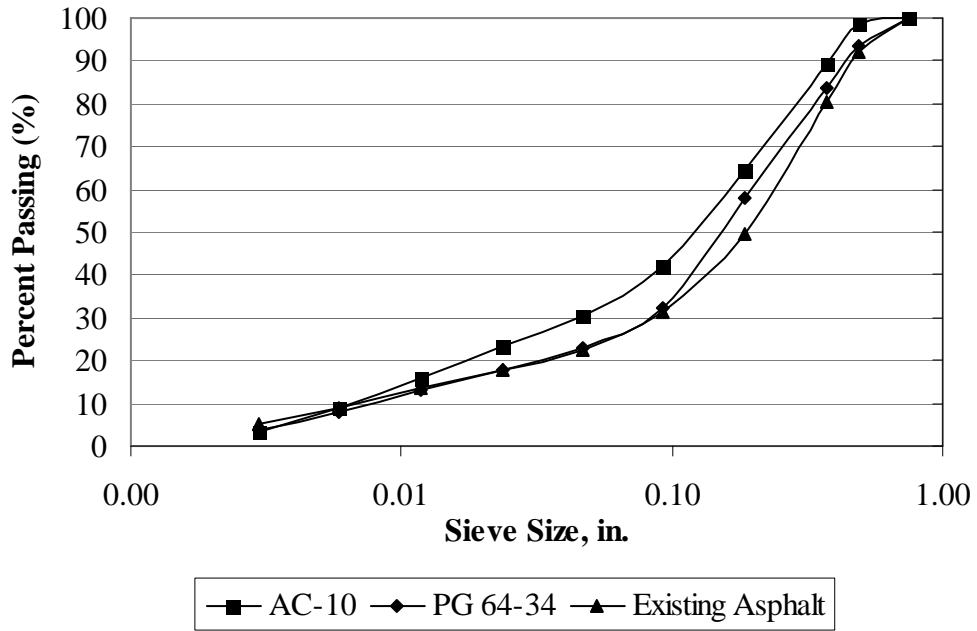


Figure 4.5 Aggregate Gradations for Asphalt Layers

4.2.2 Regression Analyses

The results of the stepwise regression analyses performed on the data collected at the conclusion of the 3-year testing period are shown in Table 4.10. A hyphen in the table indicates

Table 4.10 Results of Statistical Analyses

| Distress Type | <i>p</i> -Values | | | | | | R ² |
|-----------------------|------------------|--------------|-------------------|----------------|----------|--------------|----------------|
| | Asphalt Type | Ditch Effect | Asphalt Thickness | Base Thickness | Base CBR | Subgrade CBR | |
| Rutting | <0.001 | <0.001 | - | - | - | - | 0.337 |
| Longitudinal Cracking | - | - | - | - | 0.009 | 0.009 | 1 |
| Fatigue Cracking | 0.048 | - | - | - | 0.014 | - | 0.996 |
| Transverse Cracking | - | - | 0.007 | - | 0.006 | - | 0.999 |
| Roughness | 0.013 | - | - | - | - | - | 0.068 |

that the corresponding variable was not selected for inclusion in the given model; in such cases, the calculated *p*-values exceeded 0.15. Based on the complete statistical output given in Appendix B, statistical models were developed for each response variable for which asphalt type was a significant predictor variable. Accordingly, models for rut depth, fatigue cracking, and roughness are presented in Equations 4.1 to 4.3:

$$RD = 0.08 \cdot A - 0.06 \cdot L + 0.16 \quad (4.1)$$

where: *RD* = rut depth, in.

A = asphalt overlay type, 1.0 for AC-10 and 0.0 for PG 64-34

L = lane direction, 1.0 for eastbound and 0.0 for westbound

$$FC = -0.11 \cdot A - 0.003 \cdot B + 0.71 \quad (4.2)$$

where: *FC* = area of fatigue cracking, %

A = asphalt overlay type, 1.0 for AC-10 and 0.0 for PG 64-34

B = CBR of the base, %

$$R = -24.61 \cdot A + 94.90 \quad (4.3)$$

where: R = roughness, in./mile

A = asphalt overlay type, 1.0 for AC-10 and 0.0 for PG 64-34

Longitudinal and transverse cracking models were not developed because asphalt type, the primary variable in this research, was determined to be insignificant in those cases. As stated previously, the analyses presented in this research are applicable only to the pavements tested.

Equation 4.1 indicates that rut depths were 0.08 in. deeper, on average, in the AC-10 overlay compared to the PG 64-34 overlay. This could be attributable to superior high-temperature properties of the PG binder compared to the AC binder, but it could also be due to the use of larger aggregates in the PG product compared to the AC product. Equation 4.1 also indicates that rut depths were 0.06 in. deeper, on average, in the westbound lane compared to the eastbound lane. While this effect could result from different trafficking patterns in the two lanes, it could also be attributable to the presence of the irrigation water in the canal on the north side of the road. Water seeping into the pavement structure could have weakened the base or subgrade in the westbound lane, diminishing the pavement support there compared to that provided in the eastbound lane. As a point of reference, a rut depth of 0.5 in. signifies pavement failure (17).

Equation 4.2 indicates that fatigue cracking in the PG overlay exceeded that in the AC overlay by 0.11 percent, on average. It also suggests that fatigue cracking decreases with increasing CBR values of the base material, which is consistent with expectations; stiffer base materials reduce the magnitude of horizontal tensile strains at the bottom of the asphalt layer that

are generally responsible for the development of fatigue cracking. Fatigue cracking exceeding 20 percent of the total surface area of the pavement constitutes failure.

Equation 4.3 shows that the roughness of the PG overlay was greater by 24 in./mile, on average, than the AC overlay. No other variable significantly affected roughness.

In summary, although the AC product exhibited more rutting than the PG product, the PG product exhibited more fatigue cracking and greater roughness than the AC product. One important difference between these products is that the PG 64-34 binder contains a polymer modifier, styrene butadiene styrene (SBS), which enhances cold and warm temperature performance as shown by laboratory testing (22). After aging, however, the asphalt binder stiffens, and the improvements offered by modifiers decrease; in fact, research has shown that, after sufficient aging, modified binders perform no better than their aged unmodified counterpart (2). The stiffening resulting from asphalt modifier degradation (AMD), which occurs as the molecular size of the modifying polymer is reduced through time (23).

All research findings on AMD available in the literature are based on laboratory experiments utilizing artificial aging techniques (24); no data from field experiments specifically evaluating this effect could be identified. Nonetheless, in the current research, the SBS modifier included in the PG 64-34 overlay placed on SR-30 may have degraded and therefore allowed the mix to stiffen compared to the AC-10 overlay.

4.3 Numerical Modeling

Numerical modeling of overlay performance was accomplished using the MEPDG. Appendix C provides a full list of the inputs used to describe the project, traffic, weather, general pavement structure, wearing course structure, existing asphalt structure, base structure, and

subgrade structure. In particular, because the measured average CBR value of the base layer, which was 150, exceeded the upper bound set for CBR values in the MEPDG, the maximum allowable CBR value of 80 was chosen. Also, given the absence of specific design information about the original pavement layers, the original binder type was assumed to be AC-10, which was commonly used in that area prior to the adoption of the PG system by UDOT. Mean wheel location and mean traffic wander were determined from measurements of rut widths relative to the lane lines at the site. The MEPDG results are depicted in Figures 4.6 to 4.10.

In Figure 4.6, the apparent stepwise development of rutting through time is evident in both the observed and modeled trends; the rate of rutting is higher during summer when the asphalt temperatures are elevated and lower during winter when cold temperatures cause increased asphalt stiffness. Although the MEPDG predictions are within the range of observed rut depths, the MEPDG overestimated the AC-10 rut depth while underestimating the PG 64-34

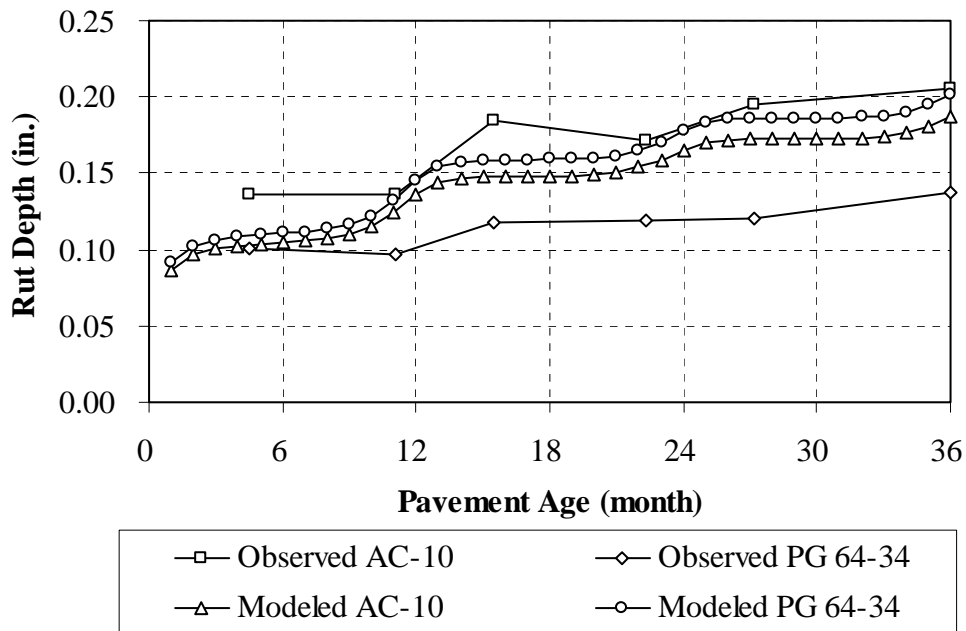


Figure 4.6 Observed and Modeled Trends in Rut Depth

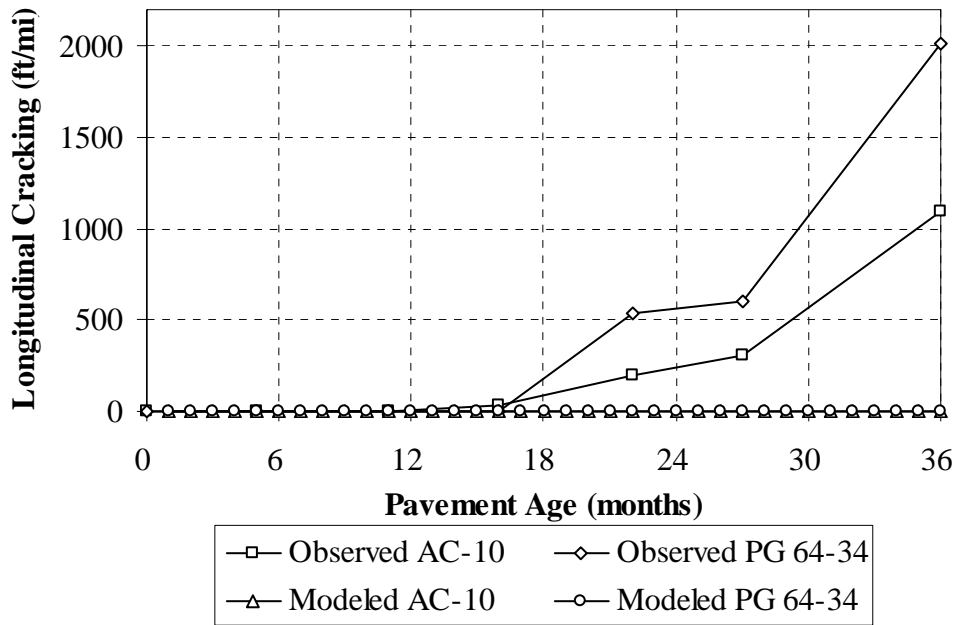


Figure 4.7 Observed and Modeled Trends in Longitudinal Cracking

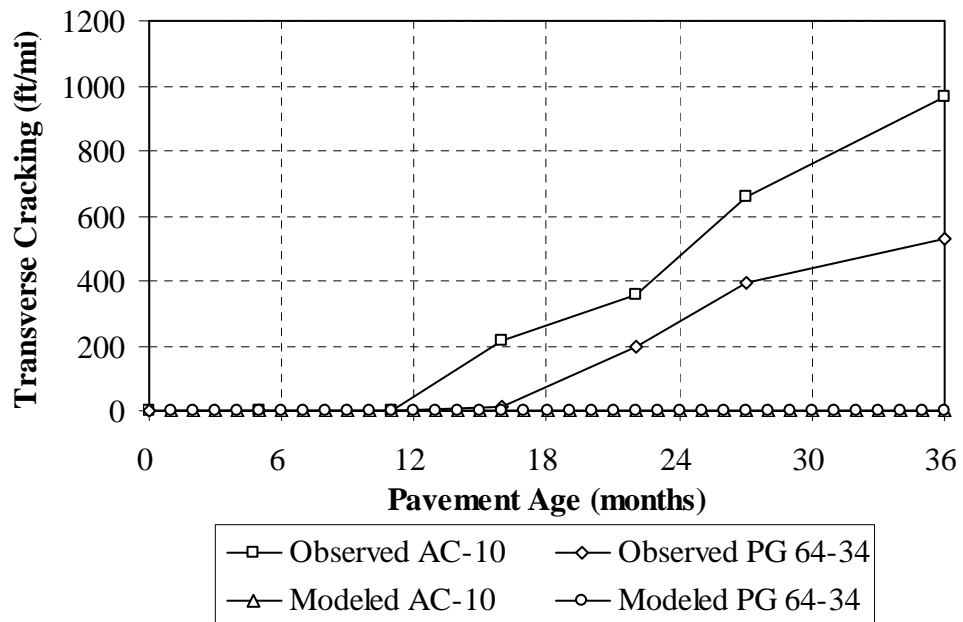


Figure 4.8 Observed and Modeled Trends in Transverse Cracking

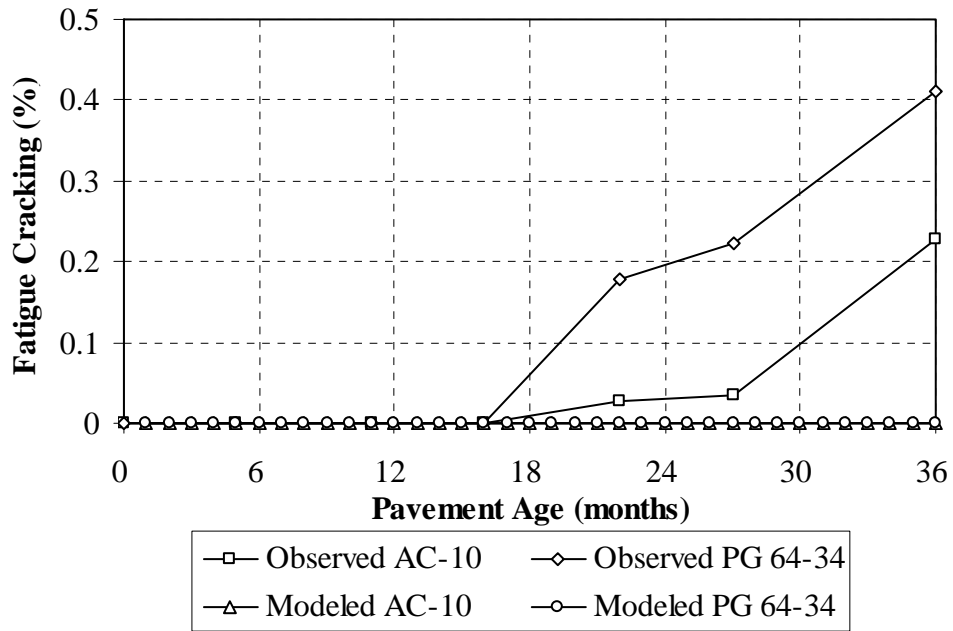


Figure 4.9 Observed and Modeled Trends in Fatigue Cracking

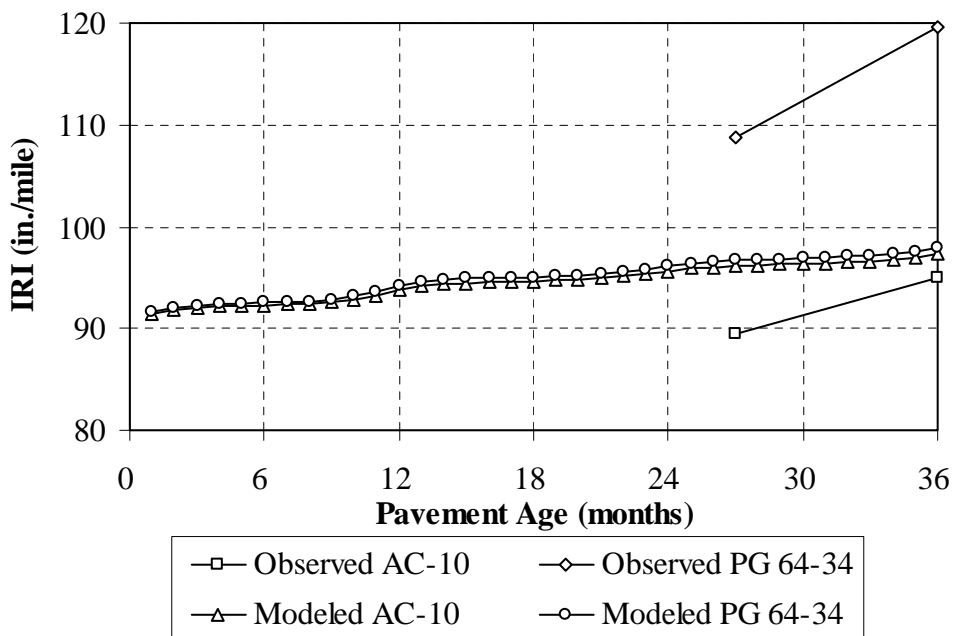


Figure 4.10 Observed and Modeled Trends in Roughness

rut depth. The largest differences between the observed and predicted values of rut depth for the AC-10 and PG 64-34 products are 0.03 and 0.06 in., respectively.

In Figure 4.7, the observed data trends show the initiation of longitudinal cracking in both types of asphalt overlays after approximately 16 months. Although a widening difference between the AC-10 and PG 64-34 products is suggested by the observed data, the statistical analyses indicated that the apparent difference is not statistically significant. While differences in observed data may not be important, the apparent inability of the MEPDG to predict comparable amounts of longitudinal cracking is concerning; the MEPDG predicted negligible longitudinal cracking for the duration of the 3-year analysis period. With the maximum predicted value from the MEPDG was 0.24 ft/mile, the largest differences between the observed and predicted values of longitudinal cracking for the AC-10 and PG 64-34 products are 1090 and 2011 ft/mile, respectively. The MEPDG longitudinal cracking model therefore appears to be deficient in the context of this research.

In Figure 4.8, a similar pattern displayed for both longitudinal and fatigue cracking is displayed for transverse cracking. Again, although a widening difference between the AC-10 and PG 64-34 products is suggested by the observed data, the statistical analyses indicated that the apparent difference is not statistically significant. A similar MEPDG prediction of negligible distress is also depicted. The largest differences between the observed and predicted values of transverse cracking for the AC-10 and PG 64-34 products are 965 and 527 ft/mile, respectively. These data suggest that the MEPDG is not suitable for predicting transverse cracking at this site.

In Figure 4.9, temporal trends in observed fatigue cracking are similar to those previously shown for longitudinal cracking, except in this case the difference in asphalt overlay products is statistically significant. Nonetheless, the MEPDG again predicts negligible distress for both

overlay types through the 3-year evaluation period. The fact that the maximum observed fatigue data only reached 0.4 percent damage across the entire test section should be considered, however. The largest differences between the observed and predicted values of fatigue cracking for the AC-10 and PG 64-34 products are only 0.23 and 0.41 percent, respectively.

In Figure 4.10, the MEPDG predictions are shown to be within the range of observed roughness values, although the MEPDG overestimated the AC-10 roughness while underestimating the PG 64-34 roughness. In this case, the observed difference in roughness between the two asphalt overlay products was determined to be both statistically significant and practically important; according to UDOT standards for high-speed asphalt shown in Table 2.1, the PG overlay is rated as “fair” after 3 years, while the AC overlay maintains a “good” rating. Nonetheless, the MEPDG results for the AC-10 and PG 64-34 products appear very similar. The largest differences between the observed and predicted values of roughness for the AC-10 and PG 64-34 products are 8 and 21 in./mile, respectively.

To investigate the possibility that the MEPDG might predict longitudinal, transverse, and fatigue cracking similar to the observed values but after a longer time period, a trial MEPDG model was constructed identical to the previous models except that the design life was extended to 20 years. However, even with an additional 17 years, the new model still predicted negligible amounts of distress.

As another approach to obtaining MEPDG results more similar to the measured distresses, the internal MEPDG climate model was adjusted. Because the behavior of an asphalt overlay is highly dependent on climatic conditions, the models within the MEPDG have climate-dependent components (20). User-definable coefficients in those components were changed in an iterative manner from the default values associated with average climatic conditions

nationwide to values ranging from the minimum to the maximum recommended inputs. Unfortunately, however, predictions of both fatigue and transverse cracking proved to be insensitive to the adjustments, and predictions of longitudinal cracking, while sensitive to the adjustments, did not change in a way that more accurately resembled the observed field data.

The lack of success in achieving improved MEPDG results through calibration is consistent with the results of a 2005 calibration study performed for the Montana Department of Transportation (MDT) in cooperation with the FHWA in an effort to locally calibrate the MEPDG to the Montana region. The authors of that study specifically indicated that the longitudinal cracking model for asphalt was insufficient. They reported, “Significant lengths of longitudinal cracking were predicted for sections with minimal longitudinal cracks, whereas no cracking was predicted for the sections with significant longitudinal cracking” (11). The authors of that study recommended that MDT use the MEPDG with caution until the MEPDG longitudinal cracking model could be revised or confirmed.

4.4 Summary

The average thicknesses of the most recent asphalt overlays, original existing asphalt, and base layers along the test section were determined from field testing to be 2.2, 9.8, and 10 in., respectively. From the measured material properties and inspection of the limited samples removed from the pavement structure during coring, the base and subgrade materials were determined to be densely compacted river gravel and clayey soil, respectively. Cores removed from the test sections clearly indicated that the roadway had been overlaid several times

Based on a complete statistical analysis, models were developed for each response variable for which asphalt type was a significant predictor variable, including rut depth, fatigue

cracking, and roughness. Longitudinal and transverse cracking models were not developed because asphalt type, the primary variable in this research, was determined to be insignificant in those cases.

At the conclusion of the 3-year evaluation period, rut depths were 0.08 in. deeper, on average, in the AC-10 overlay compared to the PG 64-34 overlay. This could be attributable to superior high-temperature properties of the PG binder compared to the AC binder, but it could also be due to the use of larger aggregates in the PG product compared to the AC product. Rut depths were 0.06 in. deeper, on average, in the westbound lane compared to the eastbound lane. While this effect could result from different trafficking patterns in the two lanes, it could also be attributable to the presence of the irrigation water in the canal on the north side of the road. Fatigue cracking in the PG overlay exceeded that in the AC overlay by 0.11 percent, on average. It also suggests that fatigue cracking decreases with increasing CBR values of the base material, which is consistent with expectations; stiffer base materials reduce the magnitude of horizontal tensile strains at the bottom of the asphalt layer that are generally responsible for the development of fatigue cracking. The measured roughness of the PG overlay was greater by 24 in./mile, on average, than the AC overlay. No other variable significantly affected roughness. In summary, although the AC product exhibited more rutting than the PG product, the PG product exhibited more fatigue cracking and greater roughness than the AC product.

Numerical modeling of overlay performance was accomplished using the MEPDG. Although the MEPDG predictions for rutting are within the range of observed rut depths, the MEPDG overestimated the AC-10 rut depth while underestimating the PG 64-34 rut depth. Furthermore, the apparent inability of the MEPDG to predict amounts of longitudinal, fatigue, and transverse cracking comparable to measured values is concerning; the MEPDG predicted

negligible cracking for both overlay types for the duration of the 3-year analysis period. While the MEPDG cracking models appear to be unsuitable for predicting cracking at this site, the MEPDG predictions for roughness are shown to be within the range of observed values, although the MEPDG overestimated the AC-10 roughness while underestimating the PG 64-34 roughness. According to UDOT standards for high-speed asphalt, the PG overlay is rated as “fair” after 3 years, while the AC overlay maintains a “good” rating.

As another approach to obtaining MEPDG results more similar to the measured distresses, the internal MEPDG climate model was adjusted. Unfortunately, however, predictions of both fatigue and transverse cracking proved to be insensitive to the adjustments, and predictions of longitudinal cracking, while sensitive to the adjustments, did not change in a way that more accurately resembled the observed field data.

5 CONCLUSION

5.1 Summary

The purpose of this research was to compare the rutting, cracking, and development of roughness of two asphalt overlay types commonly used in northern Utah and to evaluate how well the MEPDG can predict the observed results. The test sections evaluated in this research were constructed in July 2006 on SR-30 west of Logan, Utah, between mile posts 104 and 107. At this location, SR-30 consists of two lanes oriented in the east-west direction with irrigation canals along both sides of the road. PG 64-34 and AC-10 asphalt overlay materials were paved in a checkerboard pattern at the site, and 20 test stations were randomly selected along each of the east and west segments of the roadway.

Field testing involved returning to the site on approximately 6-month intervals to collect specific data from each pavement section. Primary data included rutting, cracking, and roughness, which were collected to facilitate a direct comparison of the performance of the two overlays. Material properties and layer thicknesses were evaluated as secondary data to investigate the uniformity of subsurface conditions and for use in MEPDG analyses of the test sites.

Following data collection and reduction, the effects of several factors on the performance of the overlay products at the conclusion of the 3-year testing period were investigated using statistical software. Factors of interest included overlay type, lane direction, asphalt thickness,

base thickness, and base and subgrade CBR values. A stepwise regression analysis was performed to determine the most significant predictor variables for each of the five response variables of interest in this research: rutting, fatigue cracking, longitudinal cracking, transverse cracking, and roughness.

Numerical modeling was then performed using the MEPDG. One analysis was performed for each type of asphalt overlay material, and values for the numerous inputs were determined specifically for the field sections investigated in this research. The results of the MEPDG simulations were then compared to the values of rutting, fatigue cracking, longitudinal cracking, transverse cracking, and roughness measured in the field.

5.2 Findings

The average thicknesses of the most recent asphalt overlays, original existing asphalt, and base layers along the test section were determined from field testing to be 2.2, 9.8, and 10 in., respectively. From the measured material properties and inspection of the limited samples removed from the pavement structure during coring, the base and subgrade materials were determined to be densely compacted river gravel and clayey soil, respectively.

Based on a complete statistical analysis, models were developed for each response variable for which asphalt type was a significant predictor variable, including rut depth, fatigue cracking, and roughness. Longitudinal and transverse cracking models were not developed because asphalt type, the primary variable in this research, was determined to be insignificant in those cases.

At the conclusion of the 3-year evaluation period, rut depths were 0.08 in. deeper, on average, in the AC-10 overlay compared to the PG 64-34 overlay, probably attributable to

superior high-temperature properties of the PG binder and/or the use of larger aggregates in the PG product compared to the AC product. Rut depths were 0.06 in. deeper, on average, in the westbound lane compared to the eastbound lane. While this effect could result from different trafficking patterns in the two lanes, it could also be attributable to the presence of the irrigation water in the canal on the north side of the road. Fatigue cracking in the PG overlay exceeded that in the AC overlay by 0.11 percent, on average. The measured roughness of the PG overlay was greater by 24 in./mile, on average, than the AC overlay. In summary, although the AC product exhibited more rutting than the PG product, the PG product exhibited more fatigue cracking and greater roughness than the AC product.

Although the MEPDG predictions for rutting are within the range of observed rut depths, the MEPDG overestimated the AC-10 rut depth while underestimating the PG 64-34 rut depth. Furthermore, the apparent inability of the MEPDG to predict amounts of longitudinal, fatigue, and transverse cracking comparable to measured values is concerning; the MEPDG predicted negligible cracking for both overlay types for the duration of the 3-year analysis period. While the MEPDG cracking models appear to be unsuitable for predicting cracking at this site, the MEPDG predictions for roughness are shown to be within the range of observed values, although the MEPDG overestimated the AC-10 roughness while underestimating the PG 64-34 roughness. According to UDOT standards for high-speed asphalt, the PG overlay is rated as “fair” after 3 years, while the AC overlay maintains a “good” rating.

As another approach to obtaining MEPDG results more similar to the measured distresses, the internal MEPDG climate model was adjusted. Unfortunately, however, predictions of both fatigue and transverse cracking proved to be insensitive to the adjustments, and predictions of longitudinal cracking, while sensitive to the adjustments, did not change in a

way that more accurately resembled the observed field data. As stated previously, the analyses presented in this research are applicable only to the pavements tested.

5.3 Recommendations

Given the findings of this study, the researchers recommend that UDOT engineers consider specifying the AC-10 asphalt overlay product for pavement treatments in conditions similar to those evaluated in this investigation. Although it is more susceptible to rutting than the PG 64-34 product, the AC-10 product provides a smoother ride, and it is considerably less expensive; current prices of the AC-10 and PG 64-34 overlay products are \$48 and \$75 per ton, respectively (personal communication, Blake Lubb, Staker Parson, November 20, 2009).

Even though the MEPDG predictions of rutting and roughness were reasonable for the test sections evaluated in this study, the researchers recommend that such predicted values be used as general predictions only. Further evaluation of these models, as well as the MEPDG models for longitudinal, fatigue, and transverse cracking, should be completed before the MEPDG is fully adopted by UDOT.

REFERENCES

1. Tsai, B., J. T. Harvey, and C. L. Monismith. WesTrack Fatigue Performance Prediction Using Miner's Law. In *Transportation Research Record: Journal of the Transportation Research Board*, No. 1809, Transportation Research Board of the National Academies, Washington, DC, 2002, pp. 137-147.
2. Glover, C. J., and R. J. Davison. Development of a New Method for Assessing Asphalt Binder Durability with Field Validation. Publication FHWA/TX-05/1872/2. Federal Highway Administration, Washington, DC, 2005.
3. Prowell, B. D. *Final Report: Selection and Evaluation of Performance-Graded Asphalt Binders for Virginia*. Publication VTRC 99-R21. Virginia Transportation Research Council, Virginia Department of Transportation, Charlottesville, VA, 1999.
4. Roberts, F. L., P. S. Kandhal, E. R. Brown, D. Lee, and T. W. Kennedy. *Hot Mix Asphalt Materials, Mixture, Design, and Construction*. National Asphalt Paving Association Research and Education Foundation, Lanham, MD, 1991.
5. Brown, E. R., and C. Bassett. Effects of Maximum Aggregate Size on Rutting Potential and Other Properties of Asphalt-Aggregate Mixtures. In *Transportation Research Record: Journal of the Transportation Research Board*, No. 1259, Transportation Research Board of the National Academies, Washington, DC, 1990, pp. 107-119.
6. Button, J. W., D. Perdomo, and R. L. Lytton. Influence on Aggregate Rutting of Asphalt Concrete Pavements. In *Transportation Research Record: Journal of the Transportation Research Board*, No. 1259, Transportation Research Board of the National Academies, Washington, DC, 1990, pp. 141-152.
7. Kim, S., H. Ceylan, M. Heitzman. Sensitivity Study of Design Input Parameters for Two Flexible pavement Systems using the Mechanistic-Empirical Pavement Design Guide. In *Proceedings of the 2005 Mid-Continent Transportation Research Symposium*, Iowa Department of Transportation, Ames, IA, 2005.

8. Ceylan, H., S. Kim, M. Heitzman, and K. Gopalakrishnan. Sensitivity Study of Iowa Flexible Pavements Using Mechanistic-Empirical Pavement Design Guide. In *TRB 85th Annual Meeting Compendium of Papers*. CD-ROM. Transportation Research Board of the National Academies, Washington, DC, 2006.
9. Rodezno, M. C., K. E. Kaloush, and G. B. Way. Assessment of Distress in Conventional Hot-Mix Asphalt and Asphalt–Rubber Overlays on Portland Cement Concrete Pavements: Using the New Guide to Mechanistic–Empirical Design of Pavement Structures. In *Transportation Research Record: Journal of the Transportation Research Board*, No. 1929, Transportation Research Board of the National Academies, Washington, DC, 2005, pp. 20-27.
10. Darter, M. I., L. Titus-Grover, and H. L. VonQuintus. Implementation of the Mechanistic-Empirical Design Guide in Utah: *Validation, Calibration, and Development of the UDOT MEPDG Users Guide*. Publication UT-09.11. Utah Department of Transportation, Salt Lake City, UT, 2009.
11. VonQuintus, H. L., and J. S. Moulthrop. *Mechanistic-Empirical Pavement Design Guide Flexible Pavement Performance Prediction Models Volume III Field Guide*. Publication No. FHWA/MT-07-008/8158-3. Federal Highway Administration, U.S. Department of Transportation, Washington, DC, 2007.
12. Mamlouk, M. S., and J. P. Zaniewski. *Materials for Civil and Construction Engineers, Second Edition*. Pearson Prentice Hall, Upper Saddle River, NJ, 2006.
13. Lavin, P. *Asphalt Pavements: A Practical Guide to Design, Production and Maintenance for Engineers and Architects*. Taylor & Francis, London, United Kingdom, 2003.
14. Adedimila, A. S., and A. O. Olutaiwo. Review of Advances in Grading Systems for Asphalt Binders in Hot-Mix Asphalt Pavements. *Journal of Engineering and Applied Sciences*, Vol. 4, 2008, pp. 322-331.
15. Brown, E. R., J. L. McRae, and A.B. Crawley. Effects of Aggregates on Performance of Bituminous Concrete. Implications of Aggregates in Design. *American Society of Testing and Materials*, ASTM STP 1016, Philadelphia, PA, 1989, pp 34-63.
16. Miller, J. S., and W. Y. Bellinger. *Distress Identification Manual for the Long-Term Pavement Performance Program (Fourth Revised Edition)*. Publication FHWA-RD-03-031. FHWA, U.S. Department of Transportation, Washington, DC, 2003.
17. Huang, Y. H. *Pavement Analysis and Design*. Pearson Prentice Hall, Upper Saddle River, NJ, 2004.
18. *IRI Ranges for Ride Quality and Ride Quality Index. Ride Quality*. Utah Department of Transportation, Salt Lake City, UT.
<http://www.udot.utah.gov/main/f?p=100:pg:0:::T,V:1604,>. Accessed May 12, 2009.

19. *Guide for Mechanistic Empirical Design of New and Rehabilitated Design Structures*. Final Report ERES Consultants. June 2004. <http://www.trb.org/mepdg/guide.htm>. Accessed May 12, 2009.
20. Web Soil Survey. United States Department of Agriculture (USDA). Washington, DC. <http://websoilsurvey.nrcs.usda.gov/app/WebSoilSurvey.aspx>. Accessed March 20, 2009.
21. Ramsey, F., and D. Schafer. *The Statistical Sleuth: A Course in Methods of Data Analysis 2nd Edition*. Duxbury Press, Pacific Grove, CA, 2002.
22. Airey, G. D. Styrene Butadiene Styrene Polymer Modification of Road Bitumens. *Journal of Materials Science*, Vol. 39, No. 3, 2004, pp. 951-959.
23. Lu, X., and U. Isacson. Chemical and Rheological Characteristics of Styrene-Butadiene-Styrene Polymer-Modified Bitumens. In *Transportation Research Record: Journal of the Transportation Research Board*. No. 1661, Transportation Research Board of the National Academies, Washington, DC, 1999, pp. 83-92.
24. Cortizo, M. S., D. O. Larsen, J. L. Bianchetto, and J. L. Alessandrini. Effect of Thermal Degradation of SBS copolymers during the Ageing of Modified Asphalts. *Polymer Degradation and Stability*, Vol. 86, No. 2, 2004, pp. 275-282.

APPENDIX A: RAW DATA

Table A.1 Cracking Data for November 2007

| Layer Type | Lane Direction | Transverse Cracking (ft) | | | Longitudinal Cracking (ft) | | | Fatigue Cracking (ft ²) | | |
|------------|----------------|--------------------------|--------|-----|----------------------------|--------|-----|-------------------------------------|--------|-----|
| | | High | Medium | Low | High | Medium | Low | High | Medium | Low |
| PG | WB | 0 | 0 | 0 | 0 | 4 | 0 | 0 | 0 | 0 |
| PG | EB | 0 | 0 | 17 | 0 | 0 | 0 | 0 | 0 | 0 |
| AC | WB | 0 | 106 | 72 | 0 | 0 | 25 | 0 | 0 | 0 |
| AC | EB | 0 | 54 | 10 | 0 | 0 | 8 | 0 | 0 | 0 |

Table A.2 Cracking Data for May 2008

| Layer Type | Lane Direction | Transverse Cracking (ft) | | | Longitudinal Cracking (ft) | | | Fatigue Cracking (ft ²) | | |
|------------|----------------|--------------------------|--------|-----|----------------------------|--------|-----|-------------------------------------|--------|-----|
| | | High | Medium | Low | High | Medium | Low | High | Medium | Low |
| PG | WB | 0 | 53 | 43 | 98 | 28 | 355 | 0 | 128 | 0 |
| PG | EB | 9 | 55 | 58 | 55 | 8 | 66 | 0 | 0 | 0 |
| AC | WB | 143 | 177 | 16 | 30 | 0 | 95 | 0 | 0 | 20 |
| AC | EB | 0 | 27 | 35 | 60 | 25 | 10 | 0 | 0 | 0 |

Table A.3 Cracking Data for October 2008

| Layer Type | Lane Direction | Transverse Cracking (ft) | | | Longitudinal Cracking (ft) | | | Fatigue Cracking (ft ²) | | |
|------------|----------------|--------------------------|--------|-----|----------------------------|--------|-----|-------------------------------------|--------|-----|
| | | High | Medium | Low | High | Medium | Low | High | Medium | Low |
| PG | WB | 15 | 145 | 42 | 59 | 158 | 223 | 0 | 92 | 66 |
| PG | EB | 70 | 124 | 44 | 81 | 56 | 101 | 0 | 0 | 0 |
| AC | WB | 176 | 245 | 101 | 33 | 45 | 116 | 0 | 0 | 0 |
| AC | EB | 29 | 104 | 86 | 0 | 71 | 78 | 0 | 0 | 24 |

Table A.4 Cracking Data for July 2009

| Layer Type | Lane Direction | Transverse Cracking (ft) | | | Longitudinal Cracking (ft) | | | Fatigue Cracking (ft ²) | | |
|------------|----------------|--------------------------|--------|-----|----------------------------|--------|-----|-------------------------------------|--------|-----|
| | | High | Medium | Low | High | Medium | Low | High | Medium | Low |
| PG | WB | 36 | 127 | 90 | 311 | 903 | 553 | 74 | 146 | 72 |
| PG | EB | 41 | 155 | 142 | 136 | 226 | 144 | 0 | 0 | 0 |
| AC | WB | 278 | 334 | 158 | 83 | 246 | 98 | 0 | 0 | 0 |
| AC | EB | 34 | 198 | 75 | 105 | 369 | 266 | 0 | 0 | 162 |

Table A.5 IRI Data

| Station | October 2008 | | | | July 2009 | | | |
|---------|--------------|-----|-----|-----|-----------|-----|-----|-----|
| | AC | EB | PG | WB | AC | EB | PG | WB |
| 1 | 125 | 99 | 64 | 216 | 119 | 98 | 71 | 217 |
| 2 | 117 | 79 | 87 | 288 | 137 | 95 | 83 | 312 |
| 3 | 155 | 115 | 70 | 165 | 132 | 97 | 80 | 194 |
| 4 | 129 | 124 | 103 | 104 | 138 | 121 | 110 | 101 |
| 5 | 100 | 89 | 75 | 76 | 87 | 98 | 70 | 93 |
| 6 | 76 | 68 | 70 | 89 | 90 | 74 | 61 | 110 |
| 6.5 | - | - | 67 | - | - | - | 78 | - |
| 7 | 60 | 55 | 53 | 86 | 69 | 65 | 68 | 99 |
| 8 | 71 | 84 | 88 | 126 | 51 | 103 | 95 | 128 |
| 8.5 | - | - | 54 | 103 | - | - | 39 | 113 |
| 9 | 120 | 62 | 75 | 122 | 114 | 58 | 88 | 82 |
| 10 | 122 | 63 | 94 | 111 | 119 | 81 | 109 | 131 |
| 11 | 65 | 109 | 123 | 93 | 104 | 93 | 129 | 111 |
| 12 | 70 | 107 | 73 | 106 | 127 | 123 | 59 | 112 |
| 13 | 139 | 117 | 54 | 69 | 139 | 145 | 65 | 98 |
| 13.5 | 147 | 95 | - | 70 | 133 | 112 | - | 75 |
| 14 | 79 | 142 | 50 | - | 78 | 165 | 57 | - |
| 15 | 64 | 76 | 51 | 85 | 89 | 75 | 80 | 106 |
| 16 | 79 | 68 | 83 | 105 | 65 | 65 | 114 | 104 |
| 17 | 98 | 123 | 104 | 120 | 113 | 157 | 112 | 123 |
| 17.5 | 77 | 136 | - | 96 | 67 | 159 | - | 121 |
| 18 | 54 | 57 | 66 | 79 | 40 | 83 | 54 | 159 |
| 19 | 56 | 101 | 95 | 132 | 92 | 81 | 123 | 99 |
| 20 | 89 | 211 | 269 | 132 | 70 | 274 | 286 | 160 |
| 20.5 | 68 | - | - | 108 | 67 | - | - | - |

Table A.6 Rut Depth Data for Western Sections for December 2006

| Station | Location (ft) | Westbound AC | | | | | | Eastbound PG | | | | | |
|---------|---------------|-------------------|-------------|-----------|--------------------|-------------|-----------|-------------------|-------------|-----------|--------------------|-------------|-----------|
| | | Inside Wheel Path | | | Outside Wheel Path | | | Inside Wheel Path | | | Outside Wheel Path | | |
| | | Depth (mm) | Width (in.) | | Depth (mm) | Width (in.) | | Depth (mm) | Width (in.) | | Depth (mm) | Width (in.) | |
| | | | Start Point | End Point | | Start Point | End Point | | Start Point | End Point | | Start Point | End Point |
| East | 4.0 | 5 | 0 | 41 | 4 | 0 | 42 | 2 | 0 | 44 | 6 | 0 | 59 |
| 2 | 70.0 | 5 | 0 | 35 | 4 | 0 | 40 | 4 | 0 | 38 | 3 | 0 | 26 |
| 3 | 137.0 | 3 | 0 | 30 | 4 | 0 | 36 | 3 | 0 | 30 | 3 | 0 | 19 |
| 4 | 286.0 | 4 | 0 | 36 | 2 | 0 | 72 | 3 | 0 | 24 | 2 | 0 | 44 |
| 5 | 445.0 | 7 | 0 | 34 | 3 | 0 | 30 | 3 | 0 | 25 | 2 | 0 | 23 |
| 6 | 645.5 | 4 | 0 | 30 | 4 | 0 | 35 | 2 | 0 | 27 | 3 | 0 | 34 |
| 7 | 756.0 | 5 | 0 | 33 | 5 | 0 | 32 | 3 | 0 | 44 | 2 | 0 | 35 |
| 8 | 854.0 | 8 | 0 | 36 | 3 | 0 | 25 | 3 | 0 | 34 | 3 | 0 | 33 |
| 9 | 1055.5 | 4 | 0 | 35 | 2 | 0 | 31 | 2 | 0 | 47 | 2 | 0 | 35 |
| 10 | 1215.5 | 4 | 0 | 26 | 5 | 0 | 42 | 2 | 0 | 22 | 4 | 0 | 30 |
| 11 | 1311.0 | 3 | 0 | 42 | 4 | 0 | 53 | 3 | 0 | 45 | 1 | 0 | 31 |
| 12 | 1456.0 | 7 | 0 | 62 | 4 | 0 | 50 | 4 | 0 | 26 | 5 | 0 | 40 |
| 13 | 1699.0 | 9 | 0 | 49 | 4 | 0 | 54 | 3 | 0 | 46 | 2 | 0 | 38 |
| 14 | 1815.0 | 2 | 0 | 42 | 3 | 0 | 55 | 2 | 0 | 32 | 2 | 0 | 33 |
| 15 | 2061.5 | 2 | 0 | 44 | 0 | 0 | 40 | 3 | 0 | 38 | 3 | 0 | 46 |
| 16 | 2169.0 | 4 | 0 | 43 | 3 | 0 | 52 | 3 | 0 | 28 | 2 | 0 | 29 |
| 17 | 2321.5 | 1 | 0 | 51 | 6 | 0 | 49 | 2 | 0 | 57 | 2 | 0 | 49 |
| 18 | 2470.5 | 4 | 0 | 25 | 4 | 0 | 23 | 3 | 0 | 20 | 6 | 0 | 34 |
| 19 | 2716.0 | 1 | 0 | 28 | 3 | 0 | 23 | 2 | 0 | 40 | 4 | 0 | 61 |
| 20 | 2901.0 | 3 | 0 | 23 | 2 | 0 | 33 | 6 | 0 | 36 | 2 | 0 | 33 |

Table A.7 Rut Depth Data for Eastern Sections for December 2006

| Station | Location (ft) | Westbound PG | | | | | | Eastbound AC | | | | | |
|---------|---------------|-------------------|-------------|-----------|--------------------|-------------|-----------|-------------------|-------------|-----------|--------------------|-------------|-----------|
| | | Inside Wheel Path | | | Outside Wheel Path | | | Inside Wheel Path | | | Outside Wheel Path | | |
| | | Depth (mm) | Width (in.) | | Depth (mm) | Width (in.) | | Depth (mm) | Width (in.) | | Depth (mm) | Width (in.) | |
| | | | Start Point | End Point | | Start Point | End Point | | Start Point | End Point | | Start Point | End Point |
| West | 99.0 | 1 | 0 | 26 | 3 | 0 | 32 | 2 | 0 | 18 | 2 | 0 | 28 |
| 2 | 284.0 | 2 | 0 | 30 | 1 | 0 | 27 | 2 | 0 | 22 | 3 | 0 | 36 |
| 3 | 529.5 | 1 | 0 | 23 | 2 | 0 | 28 | 2 | 0 | 33 | 6 | 0 | 39 |
| 4 | 678.5 | 2 | 0 | 17 | 2 | 0 | 20 | 4 | 0 | 32 | 4 | 0 | 37 |
| 5 | 831.0 | 1 | 0 | 18 | 2 | 0 | 29 | 2 | 0 | 30 | 7 | 0 | 43 |
| 6 | 938.5 | 1 | 0 | 34 | 2 | 0 | 33 | 3 | 0 | 32 | 2 | 0 | 22 |
| 7 | 1185.0 | 2 | 0 | 17 | 3 | 0 | 24 | 3 | 0 | 25 | 3 | 0 | 28 |
| 8 | 1301.0 | 1 | 0 | 12 | 2 | 0 | 24 | 1 | 0 | 72 | 4 | 0 | 31 |
| 9 | 1544.0 | 1 | 0 | 20 | 3 | 0 | 23 | 2 | 0 | 22 | 5 | 0 | 40 |
| 10 | 1689.0 | 3 | 0 | 19 | 3 | 0 | 21 | 2 | 0 | 30 | 4 | 0 | 38 |
| 11 | 1784.5 | 2 | 0 | 18 | 5 | 0 | 27 | 3 | 0 | 26 | 3 | 0 | 30 |
| 12 | 1944.5 | 1 | 0 | 15 | 4 | 0 | 23 | 1 | 0 | 27 | 4 | 0 | 36 |
| 13 | 2146.0 | 2 | 0 | 25 | 3 | 0 | 28 | 2 | 0 | 42 | 6 | 0 | 45 |
| 14 | 2244.0 | 2 | 0 | 16 | 3 | 0 | 22 | 2 | 0 | 31 | 5 | 0 | 55 |
| 15 | 2354.5 | 1 | 0 | 72 | 2 | 0 | 20 | 5 | 0 | 54 | 3 | 0 | 45 |
| 16 | 2555.0 | 2 | 0 | 26 | 1 | 0 | 18 | 3 | 0 | 45 | 3 | 0 | 48 |
| 17 | 2714.0 | 3 | 0 | 29 | 2 | 0 | 23 | 2 | 0 | 28 | 2 | 0 | 44 |
| 18 | 2863.0 | 2 | 0 | 23 | 3 | 0 | 26 | 2 | 0 | 26 | 3 | 0 | 25 |
| 19 | 2930.0 | 2 | 0 | 20 | 3 | 0 | 28 | 2 | 0 | 44 | 3 | 0 | 42 |
| 20 | 2996.0 | 2 | 0 | 72 | 6 | 0 | 37 | 2 | 0 | 23 | 3 | 0 | 28 |

Table A.8 Rut Depth Data for Western Sections for June 2007

| Station | Location (ft) | Westbound AC | | | | | | Eastbound PG | | | | | |
|---------|---------------|-------------------|-------------|-----------|--------------------|-------------|-----------|-------------------|-------------|-----------|--------------------|-------------|-----------|
| | | Inside Wheel Path | | | Outside Wheel Path | | | Inside Wheel Path | | | Outside Wheel Path | | |
| | | Depth (mm) | Width (in.) | | Depth (mm) | Width (in.) | | Depth (mm) | Width (in.) | | Depth (mm) | Width (in.) | |
| | | | Start Point | End Point | | Start Point | End Point | | Start Point | End Point | | Start Point | End Point |
| East | 4.0 | 4 | 6 | 50 | 4 | 3 | 57 | 2 | 20 | 38 | 6 | 5 | 73 |
| 2 | 70.0 | 3 | 6 | 48 | 4 | 14 | 52 | 2 | 14 | 67 | 5 | 1 | 49 |
| 3 | 137.0 | 3 | 7 | 49 | 3 | 7 | 70 | 1 | 15 | 39 | 2 | 8 | 43 |
| 4 | 286.0 | 8 | 1 | 51 | 1 | 6 | 48 | 2 | 15 | 53 | 2 | 19 | 46 |
| 5 | 445.0 | 7 | 3 | 49 | 3 | 15 | 42 | 2 | 10 | 45 | 0 | 0 | 0 |
| 6 | 645.5 | 3 | 9 | 48 | 3 | 11 | 50 | 2 | 5 | 50 | 0 | 0 | 0 |
| 7 | 756.0 | 5 | 2 | 52 | 4 | 6 | 51 | 1 | 19 | 47 | 1 | 25 | 44 |
| 8 | 854.0 | 5 | 7 | 52 | 6 | 2 | 58 | 2 | 5 | 43 | 0 | 0 | 0 |
| 9 | 1055.5 | 2 | 5 | 54 | 2 | 16 | 43 | 3 | 3 | 46 | 0 | 0 | 0 |
| 10 | 1215.5 | 1 | 7 | 34 | 3 | 16 | 41 | 0 | 0 | 0 | 0 | 0 | 0 |
| 11 | 1311.0 | 3 | 6 | 29 | 8 | 9 | 67 | 2 | 13 | 50 | 2 | 16 | 50 |
| 12 | 1456.0 | 6 | 2 | 54 | 4 | 8 | 47 | 4 | 8 | 63 | 3 | 20 | 54 |
| 13 | 1699.0 | 7 | 8 | 47 | 3 | 13 | 54 | 1 | 8 | 48 | 3 | 25 | 51 |
| 14 | 1815.0 | 2 | 10 | 46 | 4 | 9 | 55 | 3 | 22 | 50 | 1 | 17 | 43 |
| 15 | 2061.5 | 5 | 9 | 48 | 1 | 24 | 32 | 3 | 11 | 42 | 3 | 10 | 41 |
| 16 | 2169.0 | 6 | 3 | 43 | 4 | 5 | 68 | 0 | 0 | 0 | 3 | 8 | 52 |
| 17 | 2321.5 | 2 | 7 | 48 | 4 | 9 | 51 | 3 | 3 | 67 | 1 | 17 | 39 |
| 18 | 2470.5 | 1 | 6 | 36 | 4 | 6 | 51 | 7 | 1 | 56 | 2 | 21 | 49 |
| 19 | 2716.0 | 4 | 6 | 50 | 6 | 10 | 65 | 3 | 3 | 70 | 2 | 6 | 23 |
| 20 | 2901.0 | 3 | 34 | 58 | 2 | 37 | 64 | 3 | 44 | 66 | 3 | 35 | 67 |

Table A.9 Rut Depth Data for Eastern Sections for June 2007

| Station | Location (ft) | Westbound PG | | | | | | Eastbound AC | | | | | |
|---------|---------------|-------------------|-------------|-----------|--------------------|-------------|-----------|-------------------|-------------|-----------|--------------------|-------------|-----------|
| | | Inside Wheel Path | | | Outside Wheel Path | | | Inside Wheel Path | | | Outside Wheel Path | | |
| | | Depth (mm) | Width (in.) | | Depth (mm) | Width (in.) | | Depth (mm) | Width (in.) | | Depth (mm) | Width (in.) | |
| | | | Start Point | End Point | | Start Point | End Point | | Start Point | End Point | | Start Point | End Point |
| West | 99.0 | 5 | 24 | 62 | 1 | 16 | 37 | 2.0 | 25 | 49 | 0 | 0 | 0 |
| 2 | 284.0 | 3 | 21 | 60 | 2 | 19 | 48 | 5.0 | 19 | 52 | 0 | 0 | 0 |
| 3 | 529.5 | 2 | 24 | 47 | 0 | 0 | 0 | 5.0 | 6 | 62 | 2 | 10 | 56 |
| 4 | 678.5 | 0 | 0 | 0 | 0 | 0 | 0 | 2.0 | 31 | 54 | 2 | 18 | 37 |
| 5 | 831.0 | 3 | 20 | 51 | 0 | 0 | 0 | 3.0 | 15 | 64 | 0 | 0 | 0 |
| 6 | 938.5 | 1 | 18 | 44 | 0 | 0 | 0 | 3.0 | 17 | 47 | 3 | 18 | 54 |
| 7 | 1185.0 | 3 | 20 | 53 | 0 | 0 | 0 | 3.0 | 14 | 67 | 1 | 18 | 52 |
| 8 | 1301.0 | 3 | 22 | 49 | 0 | 0 | 0 | 4.0 | 20 | 59 | 0 | 0 | 0 |
| 9 | 1544.0 | 3 | 16 | 52 | 2 | 33 | 71 | 4.0 | 11 | 53 | 2 | 27 | 59 |
| 10 | 1689.0 | 2 | 19 | 49 | 1 | 43 | 65 | 4.0 | 19 | 51 | 1 | 19 | 49 |
| 11 | 1784.5 | 4 | 19 | 50 | 0 | 0 | 0 | 3.0 | 18 | 54 | 2 | 20 | 45 |
| 12 | 1944.5 | 5 | 9 | 51 | 1 | 49 | 70 | 3.0 | 21 | 56 | 0 | 0 | 0 |
| 13 | 2146.0 | 3 | 18 | 48 | 2 | 26 | 50 | 5.0 | 13 | 64 | 2 | 21 | 43 |
| 14 | 2244.0 | 0 | 0 | 0 | 1 | 23 | 46 | 4.0 | 57 | 72 | 3 | 2 | 52 |
| 15 | 2354.5 | 1 | 15 | 50 | 0 | 0 | 0 | 4.0 | 26 | 51 | 6 | 14 | 58 |
| 16 | 2555.0 | 1 | 24 | 39 | 0 | 0 | 0 | 4.0 | 21 | 58 | 4 | 14 | 59 |
| 17 | 2714.0 | 1 | 15 | 45 | 1 | 28 | 47 | 2.0 | 25 | 43 | 1 | 14 | 23 |
| 18 | 2863.0 | 3 | 24 | 48 | 0 | 0 | 0 | 3.0 | 16 | 47 | 4 | 53 | 70 |
| 19 | 2930.0 | 3 | 18 | 48 | 1 | 10 | 55 | 2.0 | 19 | 46 | 1 | 13 | 32 |
| 20 | 2996.0 | 5 | 24 | 58 | 2 | 21 | 46 | 4.0 | 17 | 49 | 3 | 19 | 49 |

Table A.10 Rut Depth Data for Western Sections for November 2007

| Station | Location (ft) | Westbound AC | | | | | | Eastbound PG | | | | | |
|---------|---------------|-------------------|-------------|-----------|--------------------|-------------|-----------|-------------------|-------------|-----------|--------------------|-------------|-----------|
| | | Inside Wheel Path | | | Outside Wheel Path | | | Inside Wheel Path | | | Outside Wheel Path | | |
| | | Depth (mm) | Width (in.) | | Depth (mm) | Width (in.) | | Depth (mm) | Width (in.) | | Depth (mm) | Width (in.) | |
| | | | Start Point | End Point | | Start Point | End Point | | Start Point | End Point | | Start Point | End Point |
| East | 0.0 | 5 | 4 | 48 | 6 | 4 | 58 | 3.0 | 50 | 9 | 8 | 66 | 3 |
| 2 | 66.0 | 5 | 2 | 46 | 5 | 9 | 60 | 3.0 | 53 | 3 | 9 | 53 | 3 |
| 3 | 133.0 | 3 | 7 | 50 | 5 | 16 | 68 | 3.0 | 43 | 10 | 4 | 49 | 8 |
| 4 | 281.0 | 6 | 2 | 50 | 3 | 12 | 53 | 3.0 | 51 | 15 | 4 | 46 | 19 |
| 5 | 441.0 | 8 | 4 | 46 | 4 | 7 | 49 | 2.0 | 43 | 22 | 0 | 0 | 0 |
| 6 | 695.0 | 4 | 7 | 52 | 4 | 4 | 64 | 4.0 | 49 | 7 | 2 | 59 | 11 |
| 6.5 | 761.0 | 6 | 9 | 42 | 5 | 7 | 57 | 3.0 | 16 | 50 | 2 | 21 | 48 |
| 7 | 806.0 | 8 | 2 | 51 | 7 | 10 | 51 | 2.0 | 48 | 15 | 1 | 50 | 10 |
| 8 | 904.0 | 9 | 3 | 49 | 8 | 2 | 51 | 2.0 | 8 | 40 | 1 | 22 | 51 |
| 8.5 | 1070.0 | 4 | 4 | 57 | 4 | 8 | 60 | 3.0 | 44 | 11 | 0 | 0 | 0 |
| 9 | 1105.0 | 4 | 3 | 33 | 3 | 7 | 48 | 3.0 | 7 | 48 | 2 | 26 | 55 |
| 10 | 1265.0 | 3 | 7 | 32 | 4 | 11 | 50 | 2.0 | 50 | 9 | 2 | 59 | 11 |
| 11 | 1361.0 | 4 | 2 | 34 | 9 | 9 | 65 | 3.0 | 9 | 50 | 2 | 21 | 50 |
| 12 | 1506.0 | 7 | 9 | 56 | 4 | 9 | 53 | 5.0 | 71 | 1 | 3 | 56 | 15 |
| 13 | 1736.0 | 10 | 6 | 43 | 5 | 7 | 63 | 1.0 | 10 | 35 | 3 | 17 | 52 |
| 14 | 1853.0 | 4 | 9 | 43 | 5 | 7 | 63 | 0.0 | 0 | 0 | 3 | 55 | 9 |
| 15 | 2110.0 | 7 | 9 | 53 | 3 | 16 | 64 | 2.0 | 8 | 35 | 4 | 8 | 37 |
| 16 | 2219.0 | 6 | 6 | 42 | 6 | 6 | 66 | 2.0 | 39 | 10 | 3 | 50 | 6 |
| 17 | 2371.0 | 4 | 14 | 47 | 6 | 9 | 52 | 3.0 | 6 | 37 | 1 | 16 | 38 |
| 18 | 2521.0 | 3 | 3 | 44 | 6 | 8 | 71 | 6.0 | 4 | 52 | 2 | 17 | 35 |
| 19 | 2779.0 | 6 | 4 | 49 | 7 | 11 | 65 | 3.0 | 36 | 6 | 4 | 39 | 2 |
| 20 | 2953.0 | 3 | 39 | 41 | 4 | 20 | 61 | 2.0 | 43 | 65 | 3 | 18 | 63 |

Table A.11 Rut Depth Data for Eastern Sections for November 2007

| Station | Location (ft) | Westbound PG | | | | | | Eastbound AC | | | | | |
|---------|---------------|-------------------|-------------|-----------|--------------------|-------------|-----------|-------------------|-------------|-----------|--------------------|-------------|-----------|
| | | Inside Wheel Path | | | Outside Wheel Path | | | Inside Wheel Path | | | Outside Wheel Path | | |
| | | Depth (mm) | Width (in.) | | Depth (mm) | Width (in.) | | Depth (mm) | Width (in.) | | Depth (mm) | Width (in.) | |
| | | | Start Point | End Point | | Start Point | End Point | | Start Point | End Point | | Start Point | End Point |
| West | 0.0 | 4 | 21 | 61 | 2 | 30 | 47 | 4.0 | 44 | 15 | 0 | 0 | 0 |
| 2 | 23.0 | 4 | 23 | 62 | 5 | 20 | 52 | 6.0 | 5 | 62 | 1 | 37 | 50 |
| 3 | 45.0 | 3 | 23 | 50 | 1 | 28 | 44 | 8.0 | 8 | 50 | 4 | 9 | 61 |
| 4 | 93.0 | 0 | 0 | 0 | 0 | 0 | 0 | 5.0 | 17 | 59 | 4 | 59 | 0 |
| 5 | 141.0 | 3 | 21 | 56 | 1 | 29 | 42 | 6.0 | 13 | 56 | 1 | 36 | 50 |
| 6 | 344.0 | 2 | 17 | 54 | 1 | 19 | 47 | 4.0 | 12 | 48 | 3 | 17 | 53 |
| 7 | 433.0 | 4 | 23 | 56 | 3 | 21 | 41 | 5.0 | 65 | 12 | 5 | 53 | 7 |
| 8 | 549.0 | 3 | 21 | 52 | 2 | 25 | 38 | 5.0 | 20 | 56 | 1 | 30 | 49 |
| 9 | 756.0 | 3 | 18 | 50 | 2 | 27 | 48 | 7.0 | 52 | 13 | 3 | 53 | 30 |
| 10 | 1162.0 | 3 | 14 | 53 | 0 | 0 | 0 | 5.0 | 14 | 53 | 2 | 23 | 50 |
| 11 | 1259.0 | 4 | 19 | 53 | 1 | 20 | 46 | 6.0 | 54 | 14 | 6 | 58 | 24 |
| 12 | 1403.0 | 7 | 15 | 49 | 3 | 20 | 47 | 6.0 | 17 | 64 | 1 | 30 | 44 |
| 13 | 1647.0 | 5 | 15 | 53 | 4 | 22 | 59 | 7.0 | 17 | 50 | 3 | 20 | 47 |
| 13.5 | 1772.0 | 3 | 21 | 57 | 1 | 37 | 48 | 6.0 | 10 | 56 | 1 | 32 | 51 |
| 14 | 1924.0 | 1 | 27 | 42 | 2 | 22 | 63 | 2.0 | 42 | 18 | 4 | 55 | 3 |
| 15 | 2035.0 | 5 | 22 | 50 | 3 | 8 | 51 | 4.0 | 25 | 52 | 6 | 11 | 59 |
| 16 | 2122.0 | 3 | 20 | 44 | 2 | 22 | 49 | 5.0 | 23 | 60 | 7 | 18 | 63 |
| 17 | 2279.0 | 4 | 20 | 50 | 3 | 8 | 58 | 4.0 | 52 | 10 | 3 | 56 | 8 |
| 17.5 | 2441.0 | 3 | 24 | 53 | 2 | 21 | 51 | 4.0 | 12 | 41 | 2 | 20 | 46 |
| 18 | 2615.0 | 4 | 22 | 49 | 2 | 18 | 52 | 4.0 | 43 | 9 | 3 | 57 | 22 |
| 19 | 2682.0 | 3 | 21 | 50 | 2 | 24 | 57 | 5.0 | 14 | 48 | 3 | 8 | 46 |
| 20 | 2748.0 | 6 | 14 | 58 | 2 | 14 | 39 | 4.0 | 48 | 15 | 5 | 58 | 2 |
| 20.5 | 2968.0 | 5 | 21 | 57 | 0 | 0 | 0 | 3.0 | 14 | 43 | 1 | 16 | 34 |

Table A.12 Rut Depth Data for Western Sections for May 2008

| Station | Location (ft) | Westbound AC | | | | | | Eastbound PG | | | | | |
|---------|---------------|-------------------|-------------|-----------|--------------------|-------------|-----------|-------------------|-------------|-----------|--------------------|-------------|-----------|
| | | Inside Wheel Path | | | Outside Wheel Path | | | Inside Wheel Path | | | Outside Wheel Path | | |
| | | Depth (mm) | Width (in.) | | Depth (mm) | Width (in.) | | Depth (mm) | Width (in.) | | Depth (mm) | Width (in.) | |
| | | | Start Point | End Point | | Start Point | End Point | | Start Point | End Point | | Start Point | End Point |
| East | 0.0 | 5 | 7 | 48 | 6 | 5 | 55 | 3.0 | 2 | 46 | 7 | 3 | 71 |
| 2 | 66.0 | 5 | 4 | 45 | 6 | 5 | 61 | 2.0 | 8 | 62 | 7 | 2 | 51 |
| 3 | 133.0 | 3 | 7 | 47 | 5 | 7 | 66 | 3.0 | 14 | 46 | 4 | 2 | 59 |
| 4 | 281.0 | 5 | 1 | 48 | 3 | 12 | 57 | 3.0 | 17 | 55 | 4 | 19 | 51 |
| 5 | 441.0 | 9 | 4 | 52 | 5 | 15 | 54 | 1.0 | 7 | 48 | 1 | 17 | 48 |
| 6 | 695.0 | 4 | 6 | 49 | 5 | 18 | 68 | 4.0 | 2 | 51 | 3 | 9 | 62 |
| 6.5 | 761.0 | 5 | 10 | 49 | 6 | 7 | 57 | 3.0 | 8 | 51 | 1 | 20 | 61 |
| 7 | 806.0 | 7 | 4 | 47 | 6 | 8 | 50 | 2.0 | 15 | 50 | 2 | 21 | 52 |
| 8 | 904.0 | 10 | 7 | 46 | 8 | 5 | 54 | 2.0 | 5 | 42 | 2 | 15 | 56 |
| 8.5 | 1070.0 | 5 | 7 | 55 | 4 | 10 | 62 | 3.0 | 4 | 51 | 1 | 25 | 48 |
| 9 | 1105.0 | 4 | 5 | 37 | 3 | 17 | 59 | 3.0 | 2 | 48 | 2 | 20 | 49 |
| 10 | 1265.0 | 2 | 5 | 32 | 4 | 8 | 45 | 1.0 | 7 | 55 | 2 | 14 | 59 |
| 11 | 1361.0 | 5 | 3 | 37 | 9 | 9 | 65 | 3.0 | 5 | 59 | 2 | 7 | 59 |
| 12 | 1506.0 | 5 | 3 | 43 | 4 | 14 | 50 | 5.0 | 6 | 69 | 3 | 23 | 64 |
| 13 | 1736.0 | 10 | 7 | 50 | 4 | 14 | 56 | 2.0 | 5 | 50 | 3 | 9 | 55 |
| 14 | 1853.0 | 3 | 9 | 45 | 5 | 10 | 60 | 1.0 | 13 | 52 | 2 | 11 | 49 |
| 15 | 2110.0 | 5 | 8 | 43 | 1 | 22 | 53 | 3.0 | 2 | 43 | 4 | 4 | 46 |
| 16 | 2219.0 | 7 | 6 | 40 | 5 | 7 | 69 | 3.0 | 3 | 40 | 3 | 7 | 52 |
| 17 | 2371.0 | 4 | 8 | 45 | 5 | 10 | 54 | 2.0 | 8 | 67 | 1 | 11 | 47 |
| 18 | 2521.0 | 2 | 5 | 42 | 5 | 10 | 65 | 5.0 | 2 | 68 | 3 | 19 | 45 |
| 19 | 2779.0 | 6 | 3 | 52 | 6 | 12 | 69 | 2.0 | 1 | 39 | 4 | 4 | 30 |
| 20 | 2953.0 | 3 | 17 | 57 | 3 | 39 | 64 | 3.0 | 16 | 59 | 2 | 16 | 67 |

Table A.13 Rut Depth Data for Eastern Sections for May 2008

| Station | Location (ft) | Westbound PG | | | | | | Eastbound AC | | | | | |
|---------|---------------|-------------------|-------------|-----------|--------------------|-------------|-----------|-------------------|-------------|-----------|--------------------|-------------|-----------|
| | | Inside Wheel Path | | | Outside Wheel Path | | | Inside Wheel Path | | | Outside Wheel Path | | |
| | | Depth (mm) | Width (in.) | | Depth (mm) | Width (in.) | | Depth (mm) | Width (in.) | | Depth (mm) | Width (in.) | |
| | | | Start Point | End Point | | Start Point | End Point | | Start Point | End Point | | Start Point | End Point |
| West | 0.0 | 5 | 18 | 65 | 3 | 9 | 52 | 3.0 | 17 | 56 | 1 | 19 | 33 |
| 2 | 23.0 | 5 | 20 | 65 | 5 | 13 | 53 | 5.0 | 12 | 52 | 0 | 0 | 0 |
| 3 | 45.0 | 3 | 24 | 57 | 1 | 15 | 48 | 9.0 | 7 | 66 | 5 | 4 | 58 |
| 4 | 93.0 | 2 | 28 | 57 | 2 | 37 | 64 | 3.0 | 18 | 53 | 3 | 18 | 58 |
| 5 | 141.0 | 3 | 16 | 51 | 1 | 21 | 50 | 6.0 | 11 | 63 | 2 | 34 | 49 |
| 6 | 344.0 | 4 | 13 | 51 | 2 | 14 | 44 | 4.0 | 10 | 50 | 3 | 19 | 49 |
| 7 | 433.0 | 3 | 19 | 53 | 1 | 23 | 42 | 4.0 | 11 | 69 | 5 | 9 | 55 |
| 8 | 549.0 | 4 | 21 | 53 | 3 | 18 | 44 | 4.0 | 18 | 54 | 2 | 26 | 60 |
| 9 | 756.0 | 4 | 15 | 54 | 1 | 23 | 49 | 5.0 | 9 | 55 | 2 | 22 | 53 |
| 10 | 1162.0 | 4 | 15 | 51 | 2 | 43 | 64 | 4.0 | 14 | 51 | 1 | 26 | 54 |
| 11 | 1259.0 | 4 | 17 | 51 | 1 | 24 | 50 | 5.0 | 15 | 60 | 4 | 19 | 57 |
| 12 | 1403.0 | 8 | 7 | 54 | 4 | 14 | 43 | 6.0 | 18 | 62 | 1 | 32 | 53 |
| 13 | 1647.0 | 6 | 15 | 53 | 4 | 19 | 53 | 8.0 | 17 | 61 | 3 | 20 | 50 |
| 13.5 | 1772.0 | 2 | 15 | 50 | 0 | 0 | 0 | 7.0 | 15 | 65 | 1 | 30 | 53 |
| 14 | 1924.0 | 0 | 0 | 0 | 2 | 25 | 64 | 1.0 | 17 | 44 | 3 | 8 | 53 |
| 15 | 2035.0 | 4 | 24 | 50 | 2 | 16 | 48 | 5.0 | 19 | 54 | 6 | 6 | 62 |
| 16 | 2122.0 | 1 | 21 | 43 | 0 | 0 | 0 | 4.0 | 23 | 64 | 7 | 5 | 62 |
| 17 | 2279.0 | 5 | 24 | 52 | 4 | 9 | 53 | 4.0 | 15 | 52 | 2 | 7 | 57 |
| 17.5 | 2441.0 | 3 | 14 | 49 | 0 | 0 | 0 | 4.0 | 8 | 51 | 3 | 11 | 48 |
| 18 | 2615.0 | 4 | 28 | 57 | 3 | 24 | 59 | 4.0 | 6 | 53 | 2 | 5 | 49 |
| 19 | 2682.0 | 3 | 19 | 51 | 4 | 14 | 62 | 3.0 | 14 | 51 | 2 | 9 | 48 |
| 20 | 2748.0 | 5 | 16 | 46 | 2 | 22 | 41 | 5.0 | 19 | 57 | 3 | 3 | 58 |
| 20.5 | 2968.0 | 6 | 15 | 57 | 2 | 22 | 41 | 2.0 | 11 | 47 | 1 | 13 | 40 |

Table A.14 Rut Depth Data for Western Sections for October 2008

| Station | Location (ft) | Westbound AC | | | | | | Eastbound PG | | | | | |
|-------------|---------------|-------------------|-------------|-----------|--------------------|-------------|-----------|-------------------|-------------|-----------|--------------------|-------------|----|
| | | Inside Wheel Path | | | Outside Wheel Path | | | Inside Wheel Path | | | Outside Wheel Path | | |
| | | Depth (mm) | Width (in.) | | Depth (mm) | Width (in.) | | Depth (mm) | Width (in.) | | Depth (mm) | Width (in.) | |
| Start Point | End Point | | Start Point | End Point | | Start Point | End Point | | Start Point | End Point | | | |
| East | 0.0 | 5 | 4 | 50 | 6 | 5 | 56 | 4 | 1 | 55 | 9 | 3 | 71 |
| 2 | 66.0 | 5 | 4 | 43 | 4 | 7 | 58 | 3 | 3 | 62 | 10 | 1 | 47 |
| 3 | 133.0 | 4 | 5 | 45 | 4 | 4 | 66 | 2 | 11 | 37 | 4 | 1 | 49 |
| 4 | 281.0 | 6 | 1 | 44 | 3 | 16 | 59 | 2 | 11 | 54 | 4 | 1 | 57 |
| 5 | 441.0 | 10 | 2 | 51 | 5 | 12 | 50 | 3 | 13 | 52 | 2 | 8 | 51 |
| 6 | 695.0 | 4 | 8 | 47 | 5 | 6 | 67 | 3 | 1 | 53 | 2 | 21 | 53 |
| 6.5 | 761.0 | 4 | 9 | 55 | 5 | 7 | 54 | 3 | 7 | 50 | 2 | 1 | 59 |
| 7 | 806.0 | 10 | 2 | 51 | 6 | 10 | 45 | 3 | 7 | 45 | 1 | 3 | 52 |
| 8 | 904.0 | 11 | 6 | 46 | 9 | 3 | 56 | 3 | 4 | 56 | 2 | 8 | 65 |
| 8.5 | 1070.0 | 7 | 4 | 58 | 5 | 3 | 63 | 3 | 7 | 52 | 2 | 16 | 51 |
| 9 | 1105.0 | 5 | 6 | 35 | 3 | 10 | 53 | 3 | 1 | 50 | 1 | 1 | 59 |
| 10 | 1265.0 | 1 | 4 | 29 | 4 | 9 | 47 | 2 | 6 | 57 | 3 | 4 | 61 |
| 11 | 1361.0 | 5 | 1 | 35 | 9 | 9 | 65 | 3 | 7 | 54 | 2 | 3 | 60 |
| 12 | 1506.0 | 7 | 1 | 44 | 4 | 13 | 50 | 5 | 1 | 70 | 4 | 12 | 66 |
| 13 | 1736.0 | 14 | 7 | 43 | 6 | 7 | 59 | 2 | 2 | 49 | 3 | 4 | 56 |
| 14 | 1853.0 | 6 | 13 | 44 | 7 | 6 | 63 | 1 | 1 | 71 | 4 | 2 | 64 |
| 15 | 2110.0 | 6 | 8 | 45 | 2 | 22 | 46 | 3 | 1 | 46 | 4 | 2 | 51 |
| 16 | 2219.0 | 8 | 6 | 45 | 5 | 24 | 71 | 2 | 2 | 47 | 3 | 6 | 55 |
| 17 | 2371.0 | 3 | 6 | 36 | 5 | 5 | 51 | 2 | 1 | 67 | 2 | 5 | 43 |
| 18 | 2521.0 | 4 | 6 | 34 | 5 | 7 | 70 | 6 | 1 | 68 | 2 | 9 | 48 |
| 19 | 2779.0 | 8 | 7 | 49 | 8 | 11 | 63 | 5 | 1 | 39 | 1 | 5 | 67 |
| 20 | 2953.0 | 3 | 16 | 69 | 2 | 22 | 45 | 3 | 1 | 40 | 2 | 15 | 67 |

Table A.15 Rut Depth Data for Eastern Sections for October 2008

| Station | Location (ft) | Westbound PG | | | | | | Eastbound AC | | | | | |
|---------|---------------|-------------------|-------------|-----------|--------------------|-------------|-----------|-------------------|-------------|-----------|--------------------|-------------|-----------|
| | | Inside Wheel Path | | | Outside Wheel Path | | | Inside Wheel Path | | | Outside Wheel Path | | |
| | | Depth (mm) | Width (in.) | | Depth (mm) | Width (in.) | | Depth (mm) | Width (in.) | | Depth (mm) | Width (in.) | |
| | | | Start Point | End Point | | Start Point | End Point | | Start Point | End Point | | Start Point | End Point |
| West | 0.0 | 5 | 18 | 63 | 3 | 6 | 61 | 3 | 16 | 42 | 1 | 16 | 71 |
| 2 | 23.0 | 6 | 18 | 66 | 7 | 9 | 51 | 7 | 2 | 67 | 0 | 1 | 71 |
| 3 | 45.0 | 4 | 18 | 63 | 1 | 12 | 50 | 10 | 4 | 56 | 4 | 9 | 58 |
| 4 | 93.0 | 2 | 24 | 61 | 1 | 15 | 64 | 4 | 21 | 51 | 3 | 2 | 59 |
| 5 | 141.0 | 3 | 18 | 56 | 1 | 13 | 54 | 7 | 13 | 68 | 0 | 6 | 56 |
| 6 | 344.0 | 3 | 13 | 61 | 3 | 14 | 48 | 5 | 14 | 48 | 3 | 13 | 51 |
| 7 | 433.0 | 5 | 15 | 54 | 2 | 15 | 44 | 3 | 16 | 48 | 3 | 11 | 57 |
| 8 | 549.0 | 3 | 16 | 54 | 2 | 11 | 49 | 4 | 15 | 56 | 1 | 4 | 63 |
| 9 | 756.0 | 4 | 10 | 54 | 2 | 13 | 49 | 8 | 2 | 60 | 3 | 25 | 54 |
| 10 | 1162.0 | 3 | 14 | 52 | 1 | 13 | 64 | 6 | 18 | 55 | 2 | 27 | 51 |
| 11 | 1259.0 | 4 | 17 | 55 | 2 | 8 | 45 | 6 | 14 | 55 | 3 | 7 | 49 |
| 12 | 1403.0 | 7 | 10 | 47 | 3 | 10 | 43 | 7 | 14 | 64 | 2 | 14 | 50 |
| 13 | 1647.0 | 5 | 14 | 50 | 4 | 14 | 56 | 8 | 22 | 64 | 4 | 2 | 49 |
| 13.5 | 1772.0 | 3 | 18 | 56 | 1 | 30 | 61 | 7 | 11 | 61 | 1 | 3 | 52 |
| 14 | 1924.0 | 0 | 1 | 51 | 2 | 15 | 66 | 2 | 21 | 50 | 3 | 2 | 54 |
| 15 | 2035.0 | 6 | 21 | 58 | 1 | 11 | 65 | 4 | 14 | 63 | 8 | 4 | 58 |
| 16 | 2122.0 | 2 | 18 | 51 | 1 | 15 | 56 | 6 | 17 | 64 | 9 | 3 | 61 |
| 17 | 2279.0 | 3 | 22 | 50 | 3 | 13 | 50 | 4 | 9 | 50 | 2 | 2 | 58 |
| 17.5 | 2441.0 | 1 | 24 | 47 | 1 | 15 | 57 | 4 | 7 | 44 | 3 | 12 | 45 |
| 18 | 2615.0 | 3 | 24 | 49 | 2 | 21 | 53 | 4 | 3 | 48 | 2 | 4 | 48 |
| 19 | 2682.0 | 2 | 17 | 55 | 3 | 17 | 47 | 5 | 14 | 49 | 3 | 7 | 48 |
| 20 | 2748.0 | 6 | 18 | 55 | 3 | 15 | 41 | 4 | 9 | 55 | 4 | 2 | 53 |
| 20.5 | 2968.0 | 7 | 10 | 51 | 1 | 20 | 40 | 4 | 1 | 47 | 2 | 1 | 58 |

Table A.16 Rut Depth Data for Western Sections for July 2009

| Station | Location (ft) | Westbound AC | | | | | | Eastbound PG | | | | | |
|---------|---------------|-------------------|-------------|-----------|--------------------|-------------|-----------|-------------------|-------------|-----------|--------------------|-------------|-----------|
| | | Inside Wheel Path | | | Outside Wheel Path | | | Inside Wheel Path | | | Outside Wheel Path | | |
| | | Depth (mm) | Width (in.) | | Depth (mm) | Width (in.) | | Depth (mm) | Width (in.) | | Depth (mm) | Width (in.) | |
| | | | Start Point | End Point | | Start Point | End Point | | Start Point | End Point | | Start Point | End Point |
| East | 0.0 | 6 | 3 | 54 | 7 | 4 | 57 | 3 | 1 | 52 | 10 | 2 | 71 |
| 2 | 66.0 | 7 | 2 | 46 | 6 | 3 | 62 | 3 | 8 | 62 | 11 | 1 | 51 |
| 3 | 133.0 | 4 | 2 | 49 | 6 | 3 | 69 | 4 | 11 | 43 | 4 | 2 | 57 |
| 4 | 281.0 | 7 | 1 | 51 | 3 | 2 | 67 | 2 | 13 | 50 | 3 | 4 | 53 |
| 5 | 441.0 | 7 | 4 | 51 | 10 | 1 | 52 | 2 | 4 | 45 | 1 | 5 | 52 |
| 6 | 695.0 | 4 | 2 | 52 | 6 | 3 | 68 | 3 | 7 | 54 | 1 | 6 | 60 |
| 6.5 | 761.0 | 5 | 7 | 55 | 7 | 5 | 58 | 3 | 9 | 51 | 2 | 5 | 56 |
| 7 | 806.0 | 12 | 3 | 55 | 7 | 2 | 53 | 3 | 12 | 49 | 2 | 4 | 56 |
| 8 | 904.0 | 10 | 4 | 61 | 9 | 2 | 57 | 2 | 7 | 48 | 1 | 8 | 63 |
| 8.5 | 1070.0 | 8 | 2 | 59 | 6 | 3 | 62 | 3 | 7 | 53 | 1 | 3 | 54 |
| 9 | 1105.0 | 6 | 1 | 45 | 4 | 2 | 60 | 4 | 4 | 50 | 2 | 15 | 60 |
| 10 | 1265.0 | 3 | 3 | 36 | 6 | 3 | 50 | 2 | 9 | 60 | 3 | 8 | 61 |
| 11 | 1361.0 | 4 | 3 | 49 | 9 | 8 | 67 | 3 | 6 | 55 | 4 | 6 | 50 |
| 12 | 1506.0 | 5 | 1 | 51 | 5 | 7 | 54 | 4 | 2 | 70 | 3 | 12 | 62 |
| 13 | 1736.0 | 17 | 6 | 50 | 4 | 5 | 54 | 2 | 16 | 43 | 2 | 24 | 50 |
| 14 | 1853.0 | 4 | 9 | 47 | 5 | 3 | 66 | 1 | 16 | 43 | 1 | 7 | 52 |
| 15 | 2110.0 | 7 | 6 | 48 | 1 | 18 | 57 | 1 | 2 | 43 | 4 | 4 | 47 |
| 16 | 2219.0 | 8 | 3 | 41 | 6 | 5 | 70 | 2 | 4 | 45 | 2 | 6 | 51 |
| 17 | 2371.0 | 4 | 6 | 48 | 6 | 9 | 55 | 2 | 3 | 61 | 1 | 19 | 46 |
| 18 | 2521.0 | 3 | 4 | 43 | 5 | 6 | 66 | 5 | 2 | 64 | 2 | 14 | 54 |
| 19 | 2779.0 | 6 | 4 | 52 | 7 | 12 | 67 | 1 | 17 | 61 | 3 | 2 | 34 |
| 20 | 2953.0 | 3 | 34 | 50 | 4 | 36 | 64 | 0 | 23 | 47 | 0 | 23 | 44 |

Table A.17 Rut Depth Data for Eastern Sections for July 2009

| Station | Location (ft) | Westbound PG | | | | | | Eastbound AC | | | | | |
|-------------|---------------|-------------------|-------------|-----------|--------------------|-------------|-----------|-------------------|-------------|-----------|--------------------|-------------|----|
| | | Inside Wheel Path | | | Outside Wheel Path | | | Inside Wheel Path | | | Outside Wheel Path | | |
| | | Depth (mm) | Width (in.) | | Depth (mm) | Width (in.) | | Depth (mm) | Width (in.) | | Depth (mm) | Width (in.) | |
| Start Point | End Point | | Start Point | End Point | | Start Point | End Point | | Start Point | End Point | | | |
| West | 0.0 | 8 | 15 | 67 | 4 | 13 | 51 | 4 | 15 | 57 | 1 | 15 | 37 |
| 2 | 23.0 | 7 | 13 | 58 | 9 | 11 | 52 | 7 | 6 | 57 | 1 | 14 | 50 |
| 3 | 45.0 | 6 | 15 | 62 | 1 | 18 | 51 | 11 | 3 | 61 | 6 | 2 | 59 |
| 4 | 93.0 | 3 | 20 | 57 | 2 | 14 | 67 | 5 | 11 | 57 | 3 | 1 | 60 |
| 5 | 141.0 | 4 | 13 | 52 | 2 | 18 | 53 | 7 | 6 | 60 | 2 | 29 | 51 |
| 6 | 344.0 | 3 | 17 | 48 | 3 | 14 | 46 | 5 | 10 | 58 | 4 | 13 | 55 |
| 7 | 433.0 | 7 | 15 | 56 | 3 | 16 | 49 | 5 | 13 | 65 | 3 | 6 | 57 |
| 8 | 549.0 | 4 | 18 | 55 | 5 | 12 | 52 | 7 | 15 | 58 | 2 | 2 | 51 |
| 9 | 756.0 | 5 | 13 | 57 | 3 | 17 | 48 | 9 | 15 | 54 | 3 | 22 | 52 |
| 10 | 1162.0 | 3 | 11 | 47 | 0 | 21 | 46 | 9 | 12 | 60 | 3 | 14 | 65 |
| 11 | 1259.0 | 5 | 12 | 50 | 2 | 18 | 49 | 6 | 11 | 55 | 3 | 13 | 52 |
| 12 | 1403.0 | 9 | 4 | 45 | 4 | 15 | 46 | 7 | 12 | 60 | 2 | 23 | 50 |
| 13 | 1647.0 | 8 | 12 | 50 | 5 | 18 | 55 | 8 | 12 | 57 | 4 | 14 | 50 |
| 13.5 | 1772.0 | 3 | 17 | 51 | 2 | 30 | 54 | 7 | 9 | 55 | 0 | 30 | 53 |
| 14 | 1924.0 | 2 | 27 | 44 | 3 | 22 | 68 | 2 | 12 | 43 | 3 | 4 | 57 |
| 15 | 2035.0 | 4 | 15 | 49 | 2 | 20 | 44 | 3 | 22 | 56 | 6 | 12 | 61 |
| 16 | 2122.0 | 3 | 14 | 40 | 1 | 17 | 43 | 8 | 21 | 59 | 8 | 14 | 64 |
| 17 | 2279.0 | 3 | 12 | 43 | 3 | 9 | 53 | 9 | 18 | 51 | 1 | 12 | 54 |
| 17.5 | 2441.0 | 3 | 16 | 52 | 2 | 20 | 44 | 5 | 11 | 45 | 3 | 15 | 47 |
| 18 | 2615.0 | 4 | 19 | 55 | 3 | 15 | 52 | 6 | 8 | 53 | 1 | 16 | 44 |
| 19 | 2682.0 | 3 | 17 | 55 | 4 | 13 | 51 | 5 | 15 | 51 | 1 | 15 | 46 |
| 20 | 2748.0 | 6 | 15 | 54 | 9 | 12 | 44 | 4 | 16 | 54 | 3 | 5 | 55 |
| 20.5 | 2968.0 | 5 | 7 | 54 | 2 | 20 | 43 | 3 | 15 | 46 | 1 | 12 | 51 |

APPENDIX B: RESULTS OF STATISTICAL ANALYSES

Figure B.1 Rutting Multiple Regression Summary

Subset Selection Detail Section

| Step | Action | No. of Terms | No. of X's | R2 | Term Entered | Term Removed |
|------|--------|--------------|------------|--------|--------------|--------------|
| 0 | Add | 0 | 0 | 0.0000 | Intercept | |
| 1 | Add | 1 | 1 | 0.2163 | Asphalt_0 | |
| 2 | Add | 2 | 2 | 0.3374 | Ditch_0 | |

Regression Equation Section

| Independent Variable | Regression Coefficient b(i) | Standard Error Sb(i) | T-Value to test H0:B(i)=0 | Prob Level | Reject H0 at 5%? | Power of Test at 5% |
|----------------------|-----------------------------|----------------------|---------------------------|------------|------------------|---------------------|
| Intercept | 4.0391 | 0.3137 | 12.876 | 0.0000 | Yes | 1.0000 |
| (Asphalt=AC) | 1.9768 | 0.3650 | 5.417 | 0.0000 | Yes | 0.9997 |
| (Ditch=NO) | -1.4550 | 0.3650 | -3.987 | 0.0001 | Yes | 0.9763 |

Estimated Model

$$4.03913043478261 + 1.97677865612648 * (\text{Asphalt}=\text{AC}) - 1.4550395256917 * (\text{Ditch}=\text{NO})$$

Regression Coefficient Section

| Independent Variable | Regression Coefficient | Standard Error | Lower 95% C.L. | Upper 95% C.L. | Standardized Coefficient |
|----------------------|------------------------|----------------|----------------|----------------|--------------------------|
| Intercept | 4.0391 | 0.3137 | 3.4157 | 4.6626 | 0.0000 |
| (Asphalt=AC) | 1.9768 | 0.3650 | 1.2514 | 2.7022 | 0.4728 |
| (Ditch=NO) | -1.4550 | 0.3650 | -2.1804 | -0.7297 | -0.3480 |

Note: The T-Value used to calculate these confidence limits was 1.988.

Analysis of Variance Section

| Source | DF | R2 | Sum of Squares | Mean Square | F-Ratio | Prob Level | Power (5%) |
|-----------------|----|--------|----------------|-------------|---------|------------|------------|
| Intercept | 1 | | 1664.1 | 1664.1 | | | |
| Model | 2 | 0.3374 | 132.6816 | 66.34078 | 22.148 | 0.0000 | 1.0000 |
| Error | 87 | 0.6626 | 260.5934 | 2.995327 | | | |
| Total(Adjusted) | 89 | 1.0000 | 393.275 | 4.41882 | | | |

Analysis of Variance Detail Section

| Model Term | DF | R2 | Sum of Squares | Mean Square | F-Ratio | Prob Level | Power (5%) |
|-----------------|----|--------|----------------|-------------|---------|------------|------------|
| Intercept | 1 | | 1664.1 | 1664.1 | | | |
| Model | 2 | 0.3374 | 132.6816 | 66.34078 | 22.148 | 0.0000 | 1.0000 |
| Asphalt_0 | 1 | 0.2235 | 87.87879 | 87.87879 | 29.339 | 0.0000 | 0.9997 |
| Ditch_0 | 1 | 0.1211 | 47.61213 | 47.61213 | 15.895 | 0.0001 | 0.9763 |
| Error | 87 | 0.6626 | 260.5934 | 2.995327 | | | |
| Total(Adjusted) | 89 | 1.0000 | 393.275 | 4.41882 | | | |

Fatigue B.2 Cracking Multiple Regression Summary

Subset Selection Detail Section

| Step | Action | No. of Terms | No. of X's | R2 | Term Entered | Term Removed |
|------|--------|--------------|------------|--------|--------------|--------------|
| 0 | Add | 0 | 0 | 0.0000 | Intercept | |
| 1 | Add | 1 | 1 | 0.9210 | Base_CBR | |
| 2 | Add | 2 | 2 | 0.9996 | Asphalt | |

Regression Equation Section

| Independent Variable | Regression Coefficient b(i) | Standard Error Sb(i) | T-Value to test H0:B(i)=0 | Prob Level | Reject H0 at 5%? | Power of Test at 5% |
|----------------------|-----------------------------|----------------------|---------------------------|------------|------------------|---------------------|
| Intercept | 0.7132 | 0.0141 | 50.534 | 0.0126 | Yes | 0.9999 |
| (Asphalt="PG") | -0.1131 | 0.0086 | -13.225 | 0.0480 | Yes | 0.7006 |
| Base_CBR | -0.0032 | 0.0001 | -45.539 | 0.0140 | Yes | 0.9996 |

Estimated Model

.713173716041793-.113112118944564*(Asphalt="PG")-3.18098841391066E-03*Base_CBR

Regression Coefficient Section

| Independent Variable | Regression Coefficient | Standard Error | Lower 95% C.L. | Upper 95% C.L. | Standardized Coefficient |
|----------------------|------------------------|----------------|----------------|----------------|--------------------------|
| Intercept | 0.7132 | 0.0141 | 0.5339 | 0.8925 | 0.0000 |
| (Asphalt="PG") | -0.1131 | 0.0086 | -0.2218 | -0.0044 | -0.3284 |
| Base_CBR | -0.0032 | 0.0001 | -0.0041 | -0.0023 | -1.1310 |

Note: The T-Value used to calculate these confidence limits was 12.706.

Analysis of Variance Section

| Source | DF | R2 | Sum of Squares | Mean Square | F-Ratio | Prob Level | Power (5%) |
|-----------|----|--------|----------------|--------------|----------|------------|------------|
| Intercept | 1 | | 0.1024 | 0.1024 | | | |
| Model | 2 | 0.9996 | 0.1185467 | 5.927337E-02 | 1112.937 | 0.0212 | 0.9817 |
| Error | 1 | 0.0004 | 5.325852E-05 | 5.325852E-05 | | | |

Total(Adjusted) 3 1.0000 0.1186 3.953333E-02

Analysis of Variance Detail Section

| Model Term | DF | R2 | Sum of Squares | Mean Square | F-Ratio | Prob Level | Power (5%) |
|-----------------|----|--------|----------------|--------------|----------|------------|------------|
| Intercept | 1 | | 0.1024 | 0.1024 | | | |
| Model | 2 | 0.9996 | 0.1185467 | 5.927337E-02 | 1112.937 | 0.0212 | 0.9817 |
| Asphalt | 1 | 0.0785 | 9.31498E-03 | 9.31498E-03 | 174.901 | 0.0480 | 0.7006 |
| Base_CBR | 1 | 0.9313 | 0.1104467 | 0.1104467 | 2073.785 | 0.0140 | 0.9996 |
| Error | 1 | 0.0004 | 5.325852E-05 | 5.325852E-05 | | | |
| Total(Adjusted) | 3 | 1.0000 | 0.1186 | 3.953333E-02 | | | |

Figure B.3 Roughness Multiple Regression Summary

Subset Selection Detail Section

| Step | Action | No. of Terms | No. of X's | R2 | Term Entered | Term Removed |
|------|--------|--------------|------------|--------|--------------|--------------|
| 0 | Add | 0 | 0 | 0.0000 | Intercept | |
| 1 | Add | 1 | 1 | 0.0684 | Asphalt | |

Regression Equation Section

| Independent Variable | Regression Coefficient b(i) | Standard Error Sb(i) | T-Value to test H0:B(i)=0 | Prob Level | Reject H0 at 5%? | Power of Test at 5% |
|----------------------|-----------------------------|----------------------|---------------------------|------------|------------------|---------------------|
| Intercept | 94.9049 | 6.8450 | 13.865 | 0.0000 | Yes | 1.0000 |
| (Asphalt="PG") | 24.6080 | 9.6803 | 2.542 | 0.0128 | Yes | 0.7103 |

Estimated Model

$$94.9048888888889 + 24.608 * (\text{Asphalt} = \text{"PG"})$$

Regression Coefficient Section

| Independent Variable | Regression Coefficient | Standard Error | Lower 95% C.L. | Upper 95% C.L. | Standardized Coefficient |
|----------------------|------------------------|----------------|----------------|----------------|--------------------------|
| Intercept | 94.9049 | 6.8450 | 81.3019 | 108.5079 | 0.0000 |
| (Asphalt="PG") | 24.6080 | 9.6803 | 5.3705 | 43.8455 | 0.2616 |

Note: The T-Value used to calculate these confidence limits was 1.987.

Analysis of Variance Section

| Source | DF | R2 | Sum of Squares | Mean Square | F-Ratio | Prob Level | Power (5%) |
|-----------------|----|--------|----------------|-------------|---------|------------|------------|
| Intercept | 1 | | 1034437 | 1034437 | | | |
| Model | 1 | 0.0684 | 13624.96 | 13624.96 | 6.462 | 0.0128 | 0.7103 |
| Error | 88 | 0.9316 | 185541.3 | 2108.424 | | | |
| Total(Adjusted) | 89 | 1.0000 | 199166.2 | 2237.823 | | | |

Analysis of Variance Detail Section

| Model Term | DF | R2 | Sum of Squares | Mean Square | F-Ratio | Prob Level | Power (5%) |
|-----------------------|-----------|-----------|---------------------------|------------------------|----------------|-----------------------|-----------------------|
| Intercept | 1 | | 1034437 | 1034437 | | | |
| Model | 1 | 0.0684 | 13624.96 | 13624.96 | 6.462 | 0.0128 | 0.7103 |
| Asphalt | 1 | 0.0684 | 13624.96 | 13624.96 | 6.462 | 0.0128 | 0.7103 |
| Error | 88 | 0.9316 | 185541.3 | 2108.424 | | | |
| Total(Adjusted) | 89 | 1.0000 | 199166.2 | 2237.823 | | | |

APPENDIX C: MECHANISTIC-EMPIRICAL PAVEMENT DESIGN GUIDE INPUTS

Table C.1 MEPDG Inputs for Project Information

| Input No. | Input Name | Input Value |
|-----------|--------------------------------------|-------------------------------|
| 1 | Project Name | UDOT Overlay Research Project |
| 2 | Pavement Design Life | 3 years |
| 3 | Existing Pavement Construction Month | June 1978 |
| 4 | Pavement Overlay Construction Month | July 2006 |
| 5 | Traffic Open Month | September 2006 |
| 6 | Type of Design | NONE |
| 7 | Type of Restoration | NONE |
| 8 | Type of Overlay | AC over AC |
| 9 | Project ID | UDOT Overlay |
| 10 | Section ID | AC-10 OR PG 64-34 |
| 11 | Date | July 12, 2009 |
| 12 | Station or Milepost Format | Milepost |
| 13 | Station Begin and End | Milepost 106 to Milepost 105 |
| 14 | Initial IRI (in./mi.) | 63 |
| 15 | Limit and Reliability Criteria | 80 |

Table C.2 MEPDG Inputs for Traffic Information

| Input No. | Input Name | Input Value |
|-----------|-------------------------------------------|--------------------------|
| 16 | Traffic Direction | East-West |
| 17 | Initial Two-Way AADTT | 6,045 |
| 18 | Number of Lanes in Design Direction | 1 |
| 19 | Percent of Trucks in Design Direction (%) | 22 |
| 20 | Percent of Trucks in Design Lane (%) | 100 |
| 21 | Operational Speed (mph) | 60 |
| 22 | Monthly Traffic Adjustment Factors | Default |
| 23 | Vehicle Class Distribution | Default |
| 24 | Hourly Vehicle Distribution | Default |
| 25 | Traffic Growth Factors | 6.7% Compounded Annually |
| 26 | Axle Load Distribution Factors | Default |
| 27 | Mean Wheel Location (in.) | 22.55 |
| 28 | Traffic Wander Standard Deviation (in.) | 10.5 |
| 29 | Design Lane Width (ft) | 12 |
| 30 | Number of Axles Per Truck | Default |
| 31 | Average Axle Width (ft) | 8.5 |
| 32 | Dual Tire Spacing (in.) | 13.5 |
| 33 | Tire Pressure (psi) | 100 |
| 34 | Axle Width, Tandem, Tridem, Quad (ft) | 4 |
| 35 | Short Axle Spacing | Default |
| 36 | Medium Axle Spacing | Default |
| 37 | Long Axle Spacing | Default |

Table C.3 MEPDG Inputs for Weather Information

| Input No. | Input Name | Input Value |
|-----------|---------------------------|-------------------------------|
| 38 | Weather Station | Logan-Cache Municipal Airport |
| 39 | Depth of Water Table (ft) | 2.5 |

Table C.4 MEPDG Inputs for General Pavement Structure Information

| Input No. | Input Name | Input Value |
|-----------|------------------------------------------|-------------|
| 40 | Surface Short Wave Absorptivity | 0.85 |
| 41 | HMA E* Predictive Model | NCHRP 1-37A |
| 42 | Interface Friction between Layers | 1 |
| 43 | Rehabilitation Level | Level 3 |
| 44 | Milled Thickness (in.) | 2 |
| 45 | Existing Pavement Rating | Poor |
| 46 | Total Rutting of Existing Pavement (in.) | 0 |

Table C.5 MEPDG Inputs for AC-10 Overlay Structure

| Input No. | Input Name | Input Value |
|-----------|------------------------------|-------------------------------------------------------------------------------------------------|
| 47 | Asphalt Material Type | Asphalt Concrete |
| 48 | Layer Thickness (in.) | 2 |
| 49 | Input Level | Level 3 |
| 50 | Interface Value (0 or 1) | 1 |
| 51 | Aggregate Gradation (%) | 0 retained on 3/4-in., 10.58 retained on 3/8-in., 33.89 retained on No. 4, 5.67 passing No. 200 |
| 52 | Binder Grading Type | Viscosity |
| 53 | Grade | AC-10 |
| 54 | Reference Temperature (°F) | 70 |
| 55 | Effective Binder Content (%) | 5.12 |
| 56 | Air Voids (%) | 3.65 |
| 57 | Total Unit Weight (pcf) | 144.93 |
| 58 | Poisson's Ratio | 0.35 |

Table C.6 MEPDG Inputs for PG 64-34 Overlay Structure

| Input No. | Input Name | Input Value |
|-----------|------------------------------|-------------------------------------------------------------------------------------------------|
| 47 | Asphalt Material Type | Asphalt Concrete |
| 48 | Layer Thickness (in.) | 2.25 |
| 49 | Input Level | Level 3 |
| 50 | Interface Value (0 or 1) | 1 |
| 51 | Aggregate Gradation (%) | 0 retained on 3/4-in., 16.62 retained on 3/8-in., 40.61 retained on No. 4, 5.19 passing No. 200 |
| 52 | Binder Grading Type | Superpave PG |
| 53 | Grade | PG 64-34 |
| 54 | Reference Temperature (°F) | 70 |
| 55 | Effective Binder Content (%) | 4.9 |
| 56 | Air Voids (%) | 7.68 |
| 57 | Total Unit Weight (pcf) | 139.25 |
| 58 | Poisson's Ratio | 0.35 |

Table C.7 MEPDG Inputs for Existing Asphalt Structure

| Input No. | Input Name | Input Value |
|-----------|------------------------------|----------------------------------------------------------------------------------------|
| 59 | Asphalt Material Type | Asphalt Concrete |
| 60 | Layer Thickness (in.) | 11.03 |
| 61 | Input Level | 3 |
| 62 | Interface Value (0 or 1) | 1 |
| 63 | Aggregate Gradation (%) | 0% retained on 3/4-in., 15 retained on 3/8-in, 41 retained on No. 4, 5 passing No. 200 |
| 64 | Binder Grading Type | Viscosity |
| 65 | Viscosity Grade | AC-10 |
| 66 | Reference Temperature (°F) | 70 |
| 67 | Effective Binder Content (%) | 6.34 |
| 68 | Air Voids (%) | 3.91 |
| 69 | Total Unit Weight (pcf) | 139.52 |
| 70 | Poisson's Ratio | 0.35 |

Table C.8 MEPDG Inputs for Base Structure

| Input No. | Input Name | Input Value |
|-----------|-------------------------------------------|------------------|
| 71 | Layer Thickness (in.) | 9.7 |
| 72 | Input Level | 2 |
| 73 | Poisson's Ratio | 0.35 |
| 74 | Coefficient of Lateral Earth Pressure, Ko | 0.5 |
| 75 | Layer Modulus Correlation Value | CBR of 80 |
| 76 | Unbound Material Type | River Run Gravel |

Table C.9 MEPDG Inputs for Subgrade Structure

| Input No. | Input Name | Input Value |
|-----------|-------------------------------------------|---------------|
| 77 | Layer Thickness (in.) | Semi-infinite |
| 78 | Input Level | 2 |
| 79 | Poisson's Ratio | 0.35 |
| 80 | Coefficient of Lateral Earth Pressure, Ko | 0.5 |
| 81 | Layer Modulus Correlation Value | CBR of 14.3 |
| 82 | Unbound Material Type | CL |

